Turkish Journal of Earth Sciences (Turkish J. Earth Sci.), Vol. 17, 2008, pp. 685–708. *Copyright ©TÜBİTAK*
First published online 07 April 2008

Detailed Geochemistry and K-Ar Geochronology of the Metamorphic Sole Rocks and Their Mafic Dykes from the Mersin Ophiolite, Southern Turkey

ÖMER FARUK ÇELİK

Kocaeli Üniversitesi, Mühendislik Fakültesi, Jeoloji Mühendisliği Bölümü, TR–41380 Kocaeli, Turkey
(e-mail: fcelik@kou.edu.tr)

Abstract: The metamorphic sole rocks at the base of mantle peridotites from the Mersin ophiolite consist of amphibolites and metasedimentary lithologies. Mineral parageneses in the metamorphic sole rocks exhibit amphibolite and greenschist facies assemblages. Geothermobarometric studies based on mineral assemblages and chemical compositions of minerals indicate that average metamorphic temperature during the metamorphism was 522 ± 15 °C and the pressure was less than 5 kb. Amphibolites from the metamorphic sole rocks exhibit geochemical characteristics of a supra-subduction zone (SSZ) type ophiolite, based on their major, trace and rare earth element (REE) compositions. The Th/Nb ratios of the amphibolites are higher than the average mid-ocean ridge basalt (MORB) and ocean island basalt (OIB) values. This may suggest that they were probably derived from an enriched mantle source modified by the addition of subduction component. Island arc tholeiite (IAT), OIB and MORB-like geochemistry of the amphibolites suggest that protoliths of these rocks were formed in a SSZ environment similar to the South Sandwich arc-basin system from South Atlantic ocean and the Mariana Trough from the Western Pacific. Isolated dolerite dykes intrude both the metamorphic sole rocks and the ophiolitic units at different structural levels. Dolerite dykes cutting the metamorphic sole rocks exhibit IAT-like geochemistry. They are enriched in large-ion-lithophile elements (LILE), depleted in high-field-strength elements (HFSE) and have relatively flat REE patterns, which also confirm their subduction-related origin. Double subduction is inferred here to explain the generation of the metamorphic sole rocks and dykes in the Neotethyan ocean, since the metamorphic sole rocks exhibit SSZ characteristics and were intruded by unmetamorphosed IAT-like dolerite dykes.

Key Words: ophiolite, geochemistry, metamorphic rock, dyke, East Mediterranean, Neotethys

Mersin Ofiyolitinden Metamorfik Taban Kayaçları ve Mafik Daykların Ayrıntılı Jeokimyası ve K-Ar Jeokronolojisi, Güney Türkiye

Özet: Mersin ofiyolitine ait manto peridotitlerinin tabanında yer alan metamorfik taban kayaçları amfibolitlerden ve metasedimanter litolojilerden meydana gelir. Metamorfik taban kayaçları içerisindeki mineral birliktelikleri, bu kayaçların amfibolit ve yeşilşist fasiyesi toplulukları olduğunu gösterir. Mineral topluluklarına ve minerallerin kimyasal bileşimlerine dayalı jeotermobarometre çalışmaları, metamorfizma esnasındaki metamorfik sıcaklığın 522 ± 15 °C ve basıncın 5 kb'dan az olduğuna işaret eder. Metamorfik taban kayaçlarından amfibolitlerin ana, iz ve nadir toprak elementleri bileşimlerine dayalı jeokimyası, bu kayaçların Yitim Zonu Üstü (SSZ) tipi ofiyolitlerin jeokimyasal özelliklerine sahip olduklarını gösterir. Amfibolitlerin Th/Nb oranları, ortalama değer Okyanus Ortası Sırtı Bazaltlarından (MORB) ve Okyanus Adası Bazaltlarından (OIB) yüksektir. Bu durum muhtemel olarak bu kayaçların yitim bileşeninin etkisiyle zenginleşen manto kaynağının değişmesi sonucu oluştuklarını gösterir. Amfibolitlerin Adayayı Toleyitleri (IAT), OIB ve MORB benzeri jeokimyası, bu kayaçların köken kayaçlarının Yitim Zonu Üstü ortam koşulları içerisinde oluştuklarını ve Batı Pasifikteki Mariana Trough ve Güney Atlantik Okyanusunda, Güney Sandwich yay-basen sistemlerine benzerlik sunduklarını gösterir. İzole dolerit daykları, metamorfik taban kayaçlarına ve ofiyolitik üniteye farklı yapısal seviyelerde sokulum yaparlar. Metamorfik taban kayaçlarını kesen dolerit daykları Adayayı Toleyitleri benzeri jeokimya gösterirler. Bu kayaçlar LIL elementler bakımından zenginleşmişler buna karşın HFS elementler bakımından tüketilmişlerdir. Dolerit dayklarının göreceli düz nadir toprak elementleri gidişleri de bu kayaçların yitim ile ilişkili kökenlerini teyit eder. Metamorfik taban kayaçlarının SSZ özelliklerini göstermeleri ve metamorfik olmayan Adayayı Toleyitleri benzeri dolerit daykları tarafından kesildikleri için Neotetis Okyanusunda dayklar ve metamorfik taban kayaçlarının gelişimini açıklamak için çift yitim sonucuna varılır.

Anahtar Sözcükler: ofiyolit, jeokimya, metamorfik kayaç, dayk, Doğu Akdeniz, Neotetis

Introduction

The Tauride belt, as part of the Alpine-Himalayan mountain system, is one of the best regions to observe the metamorphic sole rocks and remnants of Cretaceous ophiolites generated from the Neotethyan ocean. The ophiolites in this belt (Figure 1a) are located as dispersed slices on both sides of the Mesozoic Tauride platform carbonates (Dilek & Moores 1990; Juteau 1980). They do not exhibit a complete ophiolite stratigraphy. The deeper parts, such as tectonites, are the best preserved

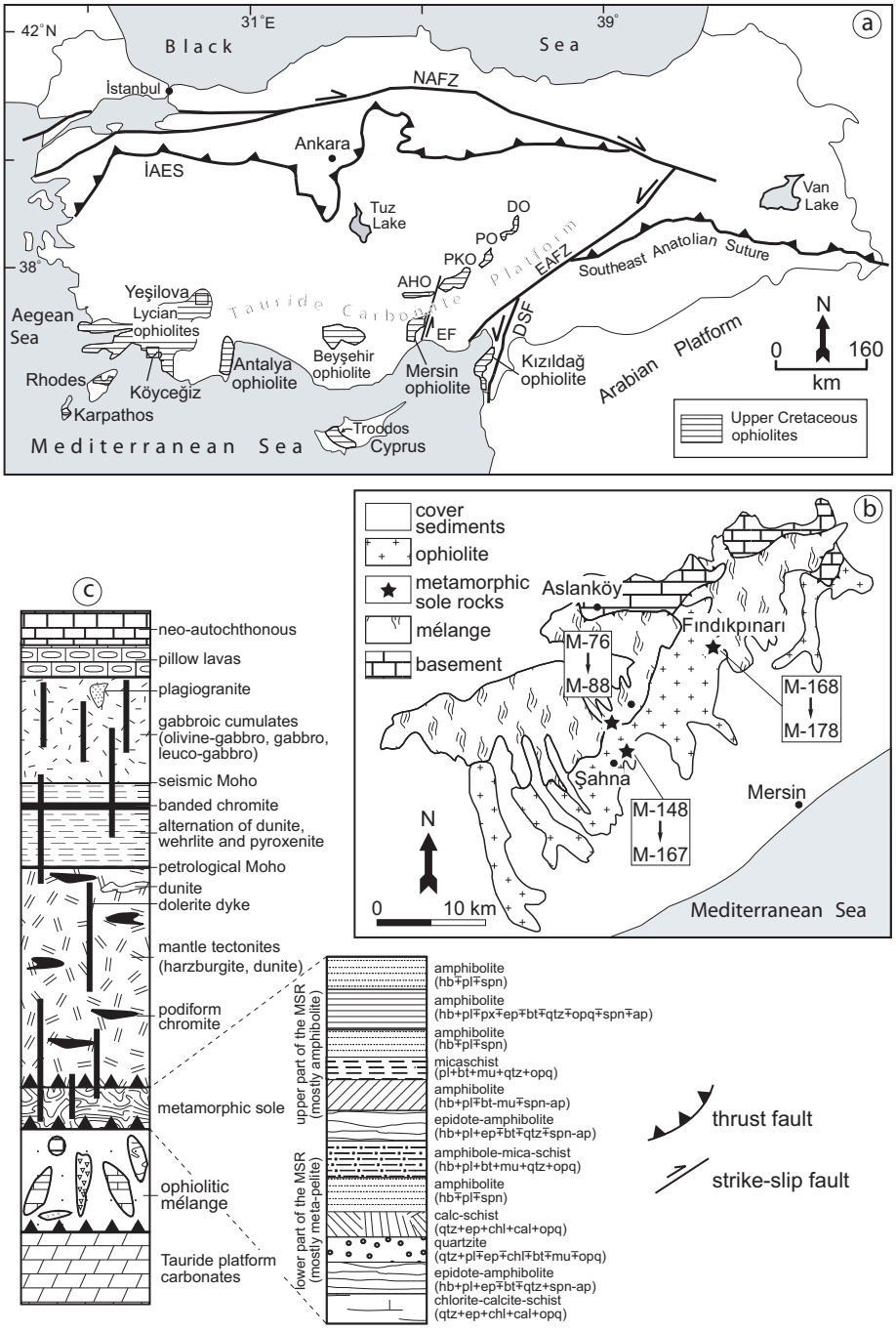

Figure 1. (a) Generalized map, modified after Dilek & Moores (1990), showing the distribution of the Tauride Belt Ophiolites and the main tectonic subdivisions of Turkey. Inset: İAES– İzmir-Ankara-Erzincan suture; NAFZ– North Anatolian Fault Zone; EAFZ– East Anatolian Fault Zone; EF– Ecemiş Fault; DSF– Dead Sea Fault; AHO– Alihoca ophiolite; PKO– Pozantı-Karsantı ophiolite; PO– Pınarbaşı ophiolite; DO– Divriği ophiolite; (b) simplified geological map of the Mersin ophiolite and the location of the samples from the metamorphic sole rocks, modified after Parlak & Delaloye (1999); (c) synthetic log of the Mersin ophiolitic complex, modified from Parlak *et al.* (1996), and the rock types of the metamorphic sole rocks (MSR). Mineral abbreviations: hb– hornblende; pl– plagioclase; px– pyroxene; ep– epidote; bt– biotite; mu– muscovite; qtz– quartz; chl– chlorite; spn– sphene; ap– apatite; cal– calcite; opq– opaque mineral.

and in the upper parts of the assemblage, sheeted dykes have generally disappeared. However, all these ophiolites contain metamorphic sole rocks and mélange units, and all these ophiolites, including the metamorphic sole rocks, are cross-cut by dolerite, gabbro and pyroxenite dykes. The isolated dolerite dykes cutting the metamorphic sole rocks are neither folded nor metamorphosed. Therefore, dyke injection has been interpreted to have occurred in an oceanic environment prior to obduction of oceanic crust onto the Tauride platform carbonates but after ductile deformation of the metamorphic sole rocks (Lytwyn & Casey 1995; Parlak & Delaloye 1996; Dilek *et al.* 1999; Çelik & Delaloye 2003).

The metamorphic sole rocks and the dykes cutting different parts of the ophiolites provide useful constraints on the age of intra-oceanic subduction and the tectonomagmatic evolution of the ophiolites in an oceanic environment. The metamorphic sole rocks from the Tauride Belt ophiolites are tectonically located between mantle peridotites and a mélange unit (Figure 1c), but can be also observed in the mélange unit as blocks of different sizes (Çelik & Delaloye 2006). The cooling and/or formation ages of the metamorphic sole rocks from the Tauride Belt ophiolites range from 91 to 93 Ma, based on ^{40}Ar-^{39}Ar geochronology (Dilek *et al.* 1999; Parlak & Delaloye 1999; Çelik *et al.* 2006). General characteristics of the metamorphic sole rocks from the Tauride Belt ophiolites are summarized in Table 1.

There are different arguments in the literature for the intra-oceanic subduction/obduction events controlling the origin of the Tauride Belt ophiolites and their metamorphic sole rocks. For example, Lytwyn & Casey (1995) and Dilek *et al.* (1999) suggested that the generation of the Tauride Belt ophiolites occurred along a mid-ocean ridge system in the Neotethyan ocean. However, many authors (e.g., Pearce *et al.* 1984; Parlak *et al.* 1996, 2000, 2002, 2006; Robertson 2002; Bağcı & Parlak 2006; Çelik *et al.* 2006) argued that generation of the ophiolites occurred in a supra-subduction zone (SSZ) environment. Also, the occurence of the metamorphic sole rocks and their dykes was mostly explained by subduction of a single oceanic lithosphere in the Neotethyan ocean (Lytwyn & Casey 1995; Polat *et al.* 1996; Parlak & Delaloye 1996, 1999; Önen & Hall 2000). Parlak *et al.* (1995) reported that, while the metamorphic sole rocks of the Mersin ophiolite exhibit within plate basalt characteristics (WPB), the dolerite dykes crosscutting the metamorphic sole rocks, as well as the Mersin ophiolite itself, present island arc tholeiite (IAT) affinities.

Backarc basins, such as the Lau and Mariana Trough from the SSZ systems of the Western Pacific ocean have a range of rock compositions that, in addition to normal mid-ocean ridge basalts (N-MORB), include IAT, backarc basin basalts (BABB), and enriched basalts that comprise ocean island basalt (OIB), as well as fractionated rocks of these series (Gribble *et al.* 1988, 1996; Hawkins 1995a, b, 2003). A similar geochemical range, from MORB to IAT, was also observed in the South Sandwich arc-basin system of South Atlantic ocean (Pearce *et al.* 2000; Leat *et al.* 2004). Accordingly, the SSZ would be a potential area to generate metamorphic sole rocks having a variety of geochemical characteristics.

This study presents geochemical and petrological characteristics of the metamorphic sole rocks and their dykes from the Mersin ophiolite. The aim of this study is to discuss possible generation of the metamorphic sole rocks in a supra-subduction zone environment.

Geological Setting

The Mersin ophiolite complex, located in the Central Tauride belt of Turkey, crops out over an area 60 km long, 25 km wide. It is separated from the Eastern Tauride belt (e.g., Pozantı-Karsantı ophiolite) by the left-lateral Ecemiş fault (Figure 1a). The Mersin ophiolite complex (~ 6 km thickness), comprises, from bottom to top (Figure 1c), the Mersin ophiolitic mélange, the metamorphic sole rocks and the Mersin ophiolite. It tectonically overlies Mesozoic platform carbonates (Juteau 1980; Dilek & Moores 1990; Parlak 1996; Parlak *et al.* 1996).

The Mersin ophiolitic mélange consists of conglomerates, sandstones, shales, mudstones, radiolarites, blocks of Permian to Cretaceous limestones, serpentinized harzburgites, gabbros, basalts, fragments of metamorphic sole rocks and granitic blocks (Parlak 1996; Parlak & Delaloye 1996, 1999; Parlak & Robertson 2004).

The metamorphic sole rocks, composed mainly of amphibolites and micaschists (Table 2), are tectonically located between the mantle tectonites and the Mersin ophiolitic mélange. Highly folded and faulted, the metamorphic sole rocks at the base of the mantle tectonites have a thickness of about 100 m. They crop out

Table 1. Geological and geochronological results from the metamorphic sole rocks and cross-cutting mafic dykes of the Tauride Belt Ophiolites.

Ophiolite	Metamorphic sole	Structural position of metamorphic sole	Age of metamorphic sole (Ma)	Protolith	Mafic dyke cutting metamorphic sole	Age of mafic dykes
LYCIAN OPHIOLITE	garnet-amphibolite, pyroxene-amphibolite, amphibolite, epidote-amphibolite, kyanite-garnet- micaschist, micaschist, marble, quartzite, (Çelik & Delaloye 2003)	tectonically located both at the base of the peridotites and in the mélange, ~ 300–350 m thickness (Çelik & Delaloye 2003)	^{40}Ar-^{39}Ar ages from Köyceğiz area (Çelik *et al.* 2006); 93.1±0.9 (hornblende) - 93.0±0.9 (hornblende), 91.7±0.7 (muscovite) - 93.6±0.8 (muscovite). ^{40}Ar-^{39}Ar ages from Yeşilova area (Çelik *et al.* 2006); 90.07±0.5 (hornblende) - 91.3±0.9 (hornblende), 91.2±2.3 (muscovite)	amphibolites: alkaline (OIB) and tholeiitic basaltic rocks (MORB, IAT). micaschist: greywackes, lithic sandstones, (Çelik 2002; Çelik & Delaloye 2003)	dolerite dykes (IAT) (Çelik & Delaloye 2003)	K-Ar ages, ranging from 63.6± 1.6 to 90.33±2.7 (Çelik 2002; Çelik & Chiaradia, 2008)
ANTALYA OPHIOLITE	pyroxene-amphibolite, amphibolite, epidote-amphibolite, (Çelik & Delaloye 2003)	tectonically located in the mélange unit (Çelik & Delaloye 2003)	^{40}Ar-^{39}Ar ages from amphibolites (Çelik *et al.* 2006); 93.0±1.0 (hornblende), 93.8±1.7 (hornblende)	amphibolites: alkaline (OIB) and tholeiitic basaltic rocks (IAT), (Çelik & Delaloye 2003)	absent	absent
BEYŞEHİR-HOYRAN OPHIOLITE	garnet-amphibolite, pyroxene-amphibolite, amphibolite, epidote-amphibolite, calc-schist, quartzite, (Çelik & Delaloye 2006)	tectonically located both at the base of the peridotites and in the mélange (Elitok 2001; Çelik & Delaloye 2006)	^{40}Ar-^{39}Ar ages from amphibolites (Çelik *et al.* 2006); 90.9±1.3 (hornblende), 91.5±1.9 (hornblende)	amphibolites: alkaline (OIB) and tholeiitic basaltic rocks (MORB), (Çelik & Delaloye 2006)	microgabbro and dolerite dykes (IAT), (Elitok 2001)	absent
POZANTI-KARSANTI OPHIOLITE	pyroxene-amphibolite, amphibolite, biotite-amphibolite, epidote-amphibolite, garnet-kyanite-amphibole micaschist, micaschist, quartzite, (Dilek *et al.* 1999; Lytwyn & Casey 1995; Polat & Casey 1996; Çelik 2007)	tectonically located both at the base of the peridotites and in the mélange, ~ 400–500 m thickness (Lytwyn & Casey 1995; Polat & Casey 1996; Dilek *et al.* 1999; Çelik 2007)	^{40}Ar-^{39}Ar ages from amphibolites (Dilek *et al.* 1999)[4]; 91.7±1.2 (hornblende), 90.4±1.8 (hornblende). ^{40}Ar-^{39}Ar ages from micaschist (Çelik *et al.* 2006); 92.4±1.3 (muscovite)	amphibolites: alkaline (OIB) and tholeiitic basaltic rocks (MORB and IAT). micaschist: lithic sandstones (Çelik 2007)	dolerite (IAT), and pyroxenite dykes (OIB), (Çelik 2007)	K-Ar ages from dolerite dykes (Thuizat et al. 1981); 71±3 (plagioclase). K-Ar (whole rock) ages from dolerite dykes (Çelik 2002); between 69.2 ±2.1 - 83.3±2.2
PINARBAŞI OPHIOLITE	amphibolite, plagioclase amphibolite, amphibole schist, epidote-plagioclase-amphibole-schist, calcschist, (Vergili & Parlak 2005)	tectonically located both at the base of the peridotites and in the mélange (Vergili & Parlak 2005)	K-Ar ages from amphibolites (Vergili & Parlak 2005); 102.2±2.9 (hornblende), 107.3±3 (hornblende)	amphibolites: OIB and IAT (Vergili & Parlak 2005)	microgabbro-diabase dykes (IAT) (Vergili & Parlak 2005)	absent
DİVRİĞİ OPHIOLITE	amphibolite, plagioclase amphibolite, plagioclase-amphibole schist, plagioclase-epidote-amphibole-schist, calcschist, (Parlak et al. 2006)	the metamorphic sole lies between mantle tectonites and mélange. ~ 100–400 m thickness (Parlak *et al.* 2006)	absent	amphibolites: alkaline (OIB) and tholeiitic (IAT) (Parlak *et al.* 2006).	dolerite dykes with alkaline affinity (OIB) (Parlak *et al.* 2006)	absent

Table 2. Mineral assemblages and textures in the metamorphic sole rocks and mafic dykes of the Mersin ophiolite.

Sample	Rock type	Texture	amp	px	pl	qtz	ep	bt	mu	chl	cal	spn	ap	opq
M-76	amphibolite	nematoblastic	X		X							X		
M-77	dolerite	sub-ophitic	X	X	X		X							X
M-78	amphibolite	decussate	X											
M-79	calcschist	granolepidoblastic				X	X	X		X	X			X
M-80	epidote-amphibolite	granonematoblastic	X		X		X				*X	X		
M-81	amphibole-quartz-micaschist	granolepidoblastic	X		X	X		X	X					X
M-82	dolerite	sub-ophitic	X		X	*X	X			X				X
M-83	amphibolite	nematoblastic	X		X		X				*X	X		
M-84	epidote-amphibolite	nematoblastic	X		X		X				*X	X		
M-85	epidote-amphibolite	nematoblastic	X		X	X	X	X		X	X			X
M-86	dolerite	micro-granular	X	X	X		X			X	*X			X
M-87	dolerite	micro-granular	X	X	X		X			X				X
M-88	chlorite-calcite-schist	granonematoblastic				X	X			X	X			X
M-148	epidote-amphibolite	nematoporphyroblastic	X		X	X	X							X
M-149	dolerite	sub-ophitic	X		X									X
M-150	dolerite	sub-ophitic	X	X	X	*X	X			X				X
M-151	amphibolite	granoblastic	X		X		*X					X	X	X
M-152	amphibolite	granoblastic	X		X							X	X	X
M-153	amphibolite	nematoblastic	X		X	X	X				X	X		X
M-154	amphibolite	granoblastic	X		X		*X					X		X
M-155	amphibolite	granoblastic	X		X							X		X
M-156	amphibolite	nematoblastic	X		X		*X					X		X
M-157	amphibolite	nematoblastic	X		X	X	X					X	X	X
M-158	amphibolite	nematoblastic	X		X		*X	X		*X				
M-159	amphibolite	granoblastic	X		X							X	X	X
M-160	epidote-amphibolite	granonematoblastic	X		X	X	X				X			X
M-161	amphibolite	granoblastic	X		X		*X	*X	*X	*X		X		X
M-162	amphibolite	granoblastic	X		X							X		
M-163	amphibolite	granoblastic	X	X	X							X		
M-164	amphibolite	nematoblastic	X		X		X	X				X		X
M-165	amphibolite	granonematoblastic	X		X							X		
M-166	amphibolite	nematoblastic	X		X		*X					X		X
M-167	amphibolite	nematoblastic	X		X							X		X
M-168	amphibolite	granonematoblastic	X		X			X				X		
M-169	amphibolite	granonematoblastic	X		X			X				X		
M-170	amphibolite	granoblastic	X		X							X	X	
M-171	amphibolite	granoblastic	X		X							X		
M-172	amphibolite	granoblastic	X		X							X		
M-173	amphibolite	granoblastic	X		X		*X					X		
M-174	amphibolite	granoblastic	X		X							X		
M-175	amphibolite	granoblastic	X		X		*X					X	X	
M-176	amphibolite	granoblastic	X	X	X		*X					X	X	X
M-177	amphibolite	granoblastic	X		X		*X			*X		X		X
M-178	amphibolite	granoblastic	X	X	X							X		

* indicating secondary mineral development (mostly in veins).

in the localities of Fındıkpınarı, Şahna and Arslanköy (Figure 1b).

The Mersin ophiolite consists of, from bottom to top, tectonized peridotites (harzburgites and dunites), ultramafic cumulates (dunite, wehrlite and pyroxenite), mafic layered cumulates (olivine gabbro, gabbro, leucogabbro and anorthosite), isotropic gabbros and minor plagiogranites, and alkaline to tholeiitic basaltic volcanics in association with deep marine sediments (Parlak 1996) (Figure 1c). The contacts in the Mersin ophiolite and surrounding units are all tectonic. Doleritic and gabbroic dykes cutting the entire ophiolite sequence and the metamorphic sole rocks do not cut the ophiolitic mélange and the platform carbonates. The Mersin ophiolite is unconformably overlain by Late Paleocene sediments (Avşar 1992).

Analytical Methods

Major and trace element analyses (Table 3) were carried out by XRF spectrometry at Lausanne University. Compositions were determined using glass beads fused in a gold-platinum crucible at 1150 °C made from ignited powders to which $Li_2B_4O_7$ had been added in a 1:5 proportion of rock to flux. Rare earth elements were analysed by inductively coupled plasma mass spectrometry (ICP-MS) at Actilabs, in Ancaster, Ontario). Detection limits (ppm) and Analytical Uncertainty (%) of the following elements are: Sc (1.2 ppm, 6.6%), V (1.2 ppm, 3.1%), Cr (1.1 ppm, 7.4%), Co (1 ppm, 19.4%), Ni (0.9 ppm, 8.1%), Cu (1.1 ppm, 19.6%), Zn (1.1 ppm, 3.8%), Ga (0.5 ppm, 9.2%), Rb (0.6 ppm, 3.1%), Sr (0.8 ppm, 3.4%), Y (0.8 ppm, 1.6%), Zr (0.7 ppm, 2.4%), Nb (0.6 ppm, 5.8%), Ba (7 ppm, 11.4%), Hf (0.7 ppm, 16.6%), Pb (1.1 ppm, 8.2%), Th (1.4 ppm, 5.7%), U (0.7 ppm, 22.6%).

Mineral analyses were performed on a Cameca SX50 electron microprobe at University of Lausanne equipped with wavelength dispersive spectrometry. Operating conditions were 15kV accelerating voltage and 15 nA sample current. Counting times of 10–30 s were applied. The amphibole analyses were re-calculated by using a spreadsheet program of Tindle & Webb (1994). Results of mineral analyses are given in Tables 4–7.

K-Ar age measurements were performed at the Geneva University (Switzerland) Mineralogy Department. The extracted minerals were obtained by magnetic separation, heavy liquids and hand picking under a binocular microscope in order to produce high-purity mineral separates (>99%). Potassium concentrations were measured twice using atomic absorption (Pye-Unicam 8000). The values reported in Table 8 are therefore the average of the duplicate measurements. Isotope analyses of argon were made using isotope dilution on an AEI-10-S mass spectrometer. Constants were those recommended by Steiger & Jäger (1977). LP-6 and HD-B1 international standards were used for calibration of the mass spectrometer response.

Mineralogy and Petrography

The upper part of the metamorphic sole rocks (close to the mantle tectonites) consists mainly of amphibolites, whereas the lower part comprises mica schists, calcschists, marble and quartzite. The mica schists were also observed as small slices within the amphibolites, as observed in the Pozantı-Karsantı and Lycian ophiolites (Çelik 2002, 2007; Çelik & Delaloye 2003). The foliation in the amphibolites is common and defined by subparallel alignment of amphibole-epidote and amphibole-plagioclase crystalloblasts. The commonest textures of the amphibolites are granoblastic, nematoblastic and granonematoblastic.

Based on the classification of Leake *et al*. (1997), all amphiboles in the amphibolites and dolerite dykes are calcic amphiboles. Amphibole compositions (edenite and magnesio-hornblende) from the amphibolites are characterized by SiO_2= (44.8–46.8 %), Al_2O_3= (8.7–11.1 %), FeO= (12.7–14.7 %), MgO= (11.5–12.7 %) and K_2O= (0.5–0.8 %). X_{Mg} values ($Mg/Mg+Fe^{+2}$) of amphiboles range from 0.58 to 0.67 (Table 4). Pyroxene in the amphibolites (M-178) was observed as equidimensional crystalloblasts. In sample (M-178) it is represented by diopside with Al (0.08–0.1 a.p.f.u.) and Na (0.04 a.p.f.u.) contents and a higher Si content (1.95–1.97 a.p.f.u.). Titanite and apatite are the most abundant accessory minerals in the parageneses. Titanite was commonly observed along the foliation planes and as inclusions in the amphibole crystalloblasts. It is also parallel to the lineation orientation of the amphibole crystalloblast and may be developed during the deformation stage of the metamorphic sole rocks. Plagioclase is commonly altered to saussurite and sericite and generally lacks polysynthetic twinning. Plagioclases from the amphibolite (M-154) have

Table 3. Chemical analyses of amphibolites. meta-pelites and dolerite dykes from the metamorphic sole rocks of the Mersin ophiolite.

Sample	M-76	M-78	M-80	M-83	M-85	M-148	M-151	M-153	M-154	M-157	M-159	M-164	M-165	M-168	M-170	M-171	M-175	M-176	M-178
Rock type	amp	amp	amp	amp	amp	amp	amp	amp	amp	amp	amp	amp	amp	amp	amp	amp	amp	amp	amp
SiO_2	45.82	41.70	37.32	44.07	35.94	43.63	44.97	45.03	44.93	46.62	44.36	46.84	44.71	43.92	43.26	44.52	43.52	45.02	43.72
Al_2O_3	11.09	11.00	13.47	11.59	12.40	13.72	11.47	15.30	11.50	16.04	11.81	15.58	11.96	11.93	12.28	12.73	12.06	13.25	11.96
TiO_2	2.30	1.15	2.26	1.69	2.09	3.22	2.87	3.39	2.90	3.27	3.03	2.49	3.02	2.61	2.59	2.49	2.39	3.41	2.58
$Fe_2O_3(T)$*	12.45	14.26	9.98	11.31	9.90	13.80	13.91	14.39	13.59	14.03	14.48	13.04	13.79	13.85	14.57	13.80	13.46	13.13	14.06
MnO	0.19	0.20	0.16	0.14	0.16	0.19	0.18	0.18	0.18	0.17	0.18	0.17	0.19	0.19	0.23	0.20	0.20	0.25	0.19
MgO	12.45	18.08	4.57	9.27	7.61	9.44	10.64	7.56	10.68	5.85	10.36	7.62	10.33	11.14	10.58	10.41	11.79	6.83	11.53
CaO	12.37	8.07	24.01	14.89	17.03	11.54	11.59	7.87	11.97	7.25	11.39	8.76	12.28	12.14	11.92	11.43	11.81	12.29	12.04
Na_2O	1.61	1.10	0.92	2.47	1.38	2.62	2.41	3.73	2.37	4.78	2.53	3.96	2.01	2.18	2.25	2.33	2.25	2.58	2.15
K_2O	0.75	0.13	0.15	0.32	1.89	0.45	0.67	0.62	0.52	0.65	0.70	0.71	0.81	0.75	0.87	1.24	0.70	1.86	0.70
P_2O_5	0.34	0.10	0.29	0.24	0.22	0.59	0.36	0.48	0.34	0.49	0.39	0.37	0.40	0.38	0.30	0.36	0.35	0.69	0.38
Cr_2O_3	0.11	0.19	0.05	0.11	0.04	0.05	0.11	0.04	0.11	0.01	0.09	0.02	0.09	0.10	0.10	0.09	0.09	0.04	0.10
NiO	0.06	0.10	0.02	0.07	0.02	0.04	0.03	0.02	0.03	0.01	0.03	0.02	0.03	0.04	0.03	0.04	0.04	0.02	0.04
LOI	0.97	3.66	7.15	4.43	11.88	1.17	0.64	1.31	1.09	1.04	0.73	0.96	0.84	0.91	0.81	0.86	1.01	0.96	0.93
Total	100.51	99.74	100.33	100.59	100.55	100.46	99.84	99.91	100.21	100.22	100.09	100.53	100.47	100.13	99.79	100.49	99.66	100.33	100.37
ppm																			
Sc	44	51	8	24	15	31	51	36	42	24	37	35	38	45	46	41	45	20	47
V	244	214	183	216	188	315	303	262	306	210	318	245	302	276	290	285	278	238	284
Cr	774	1292	287	684	309	306	762	234	721	55	620	141	611	694	709	645	678	225	730
Co	69	95	54	76	47	73	64	61	73	59	67	55	71	69	64	69	67	55	68
Ni	406	664	150	439	100	270	222	193	234	64	210	119	224	265	244	247	264	116	283
Cu	64	42	52	80	72	94	83	53	73	2	124	52	84	87	142	101	50	57	88
Zn	97	102	68	93	88	110	107	111	106	124	115	102	114	105	120	110	106	112	109
Ga	16	14	14	13	15	19	17	20	17	22	18	19	18	17	17	15	16	19	16
Rb	15	6	5	6	33	8	14	13	7	14	13	12	14	10	10	19	9	28	9
Sr	352	20	450	214	153	467	208	434	434	487	376	564	329	276	195	299	242	646	258
Y	22	13	17	17	17	24	21	24	21	28	23	23	22	22	24	21	21	27	22
Zr	159	50	203	104	192	206	178	216	173	213	189	138	188	149	151	146	153	318	147
Nb	34	12	40	25	39	60	41	35	39	46	43	31	42	36	36	33	34	73	35
Ba	101	15	n.d	54	136	205	212	215	87	172	408	229	157	145	130	401	176	1138	104
Hf	n.d	n.d	3	n.d	7	n.d	3	5	2	4	3	2	3	n.d	n.d	n.d	2	11	n.d
Pb	12	16	6	8	n.d	5	7	4	7	n.d	6	5	7	6	6	6	6	n.d	7
Th	5	4	6	4	6	5	8	5	5	4	6	3	7	5	3	5	5	9	4
U	2	2	4	2	2	2	4	2	n.d	2	2	n.d	2	2	n.d	3	2	3	2
La	24.79	2.79	24.48	19.48	25.40					2.64								66.89	
Ce	54.16	8.75	53.06	39.59	54.14					8.33								137.78	
Pr	6.65	1.26	6.11	4.79	6.18					1.43								15.57	
Nd	27.64	6.25	25.02	20.16	24.74					7.93								61.34	
Sm	5.87	2.05	5.38	4.56	5.16					2.91								11.79	
Eu	1.83	0.76	1.88	1.33	1.51					0.93								3.17	
Gd	5.32	2.18	4.80	4.15	4.25					3.62								9.13	
Tb	0.75	0.36	0.68	0.60	0.60					0.65								1.21	
Dy	4.27	2.21	3.84	3.46	3.41					4.52								6.47	
Ho	0.79	0.43	0.72	0.63	0.62					0.98								1.14	
Er	2.08	1.17	1.89	1.64	1.61					2.94								2.92	
Tm	0.27	0.16	0.26	0.22	0.22					0.45								0.38	
Yb	1.69	0.98	1.57	1.25	1.36					2.93								2.25	
Lu	0.24	0.14	0.22	0.17	0.19					0.45								0.32	

n.d = not detected. amp = amphibolite. * = Total iron expressed as Fe_2O_3.

Table 3. (Continued)

Sample Rock type	M-77 dolerite dyke	M-82 dolerite dyke	M-86 dolerite dyke	M-87 dolerite dyke	M-149 dolerite dyke	M-150 dolerite dyke	M-79 micaschist	M-81 micaschist	M-88 micaschist
SiO_2	52.45	53.54	51.87	51.39	53.52	52.04	26.62	76.00	49.43
Al_2O_3	15.92	15.76	15.13	16.11	15.86	15.46	1.62	9.05	14.61
TiO_2	0.73	1.29	0.46	0.78	1.15	1.26	9.73	0.88	0.71
Fe_2O_3(T)*	9.93	11.85	8.57	9.87	11.67	11.58	6.42	5.86	8.96
MnO	0.16	0.18	0.15	0.16	0.19	0.18	0.12	0.06	0.23
MgO	6.38	4.26	8.25	6.19	5.13	5.05	3.42	2.20	5.30
CaO	9.94	7.47	9.47	9.23	8.12	7.67	27.50	0.93	7.77
Na_2O	1.75	3.01	1.49	1.83	2.63	3.37	1.38	1.26	2.98
K_2O	0.75	0.90	1.66	1.93	0.99	1.13	2.13	2.51	1.21
P_2O_5	0.06	0.12	0.04	0.07	0.10	0.11	0.29	0.12	0.06
Cr_2O_3	0.02	0.00	0.05	0.03	0.01	0.01	20.64	0.01	0.02
NiO	0.01	0.00	0.02	0.01	0.00	0.00	0.03	0.01	0.01
LOI	1.87	1.66	2.74	2.28	0.61	1.40	0.02	1.12	8.66
Total	99.95	100.04	99.89	99.87	99.99	99.26	99.91	100.00	99.96
ppm									
Sc	40	38	35	35	40	43	n.d	8	40
V	302	368	247	316	379	375	132	94	248
Cr	118	16	239	127	21	33	280	38	149
Co	54	54	50	46	55	47	44	69	42
Ni	58	15	106	59	21	31	86	36	45
Cu	70	33	66	67	40	31	9	41	28
Zn	70	91	63	72	89	88	85	68	159
Ga	15	18	13	15	16	17	11	12	16
Rb	24	20	31	39	25	25	46	49	31
Sr	128	182	62	109	152	163	172	53	164
Y	19	27	16	21	26	27	14	19	18
Zr	38	79	25	44	63	70	192	114	43
Nb	2	4	1	2	4	4	31	28	7
Ba	53	174	337	1144	137	129	161	425	168
Hf	3	6	n.d	n.d	5	n.d	n.d	10	n.d
Pb	12	8	10	9	10	9	n.d	14	10
Th	3	n.d	3	3	3	n.d	8	9	n.d
U	2	n.d	n.d	3	2	n.d	10	2	n.d
La	3.76	3.29	0.72	2.07	2.25	2.83			
Ce	6.16	9.84	2.19	5.20	7.15	8.70			
Pr	0.99	1.66	0.37	0.89	1.24	1.48			
Nd	5.04	9.16	2.27	4.84	6.92	8.19			
Sm	1.75	3.25	1.01	1.78	2.56	2.92			
Eu	0.57	1.03	0.40	0.66	0.86	0.95			
Gd	2.20	3.96	1.51	2.34	3.34	3.70			
Tb	0.41	0.71	0.29	0.43	0.61	0.66			
Dy	2.93	4.92	2.09	3.12	4.26	4.61			
Ho	0.65	1.08	0.47	0.69	0.94	1.01			
Er	2.04	3.22	1.47	2.11	2.84	3.05			
Tm	0.31	0.48	0.22	0.33	0.43	0.45			
Yb	2.09	3.25	1.52	2.15	2.88	3.03			
Lu	0.33	0.51	0.23	0.34	0.44	0.47			

Table 4. Amphibole analyses from the amphibolites of the metamorphic sole rocks of the Mersin ophiolite.

Sample	M-154-1c	M-154-3c	M-154-4c	M-154-5c	M-154-5r	M-154-5r1	M-154-6c	M-154-7c	M-154-8c	M-154-9c	M-154-10c	M-151-1c	M-151-1r	M-151-2c	M-151-3c	M-151-4c
SiO_2	45.98	46.71	46.04	46.61	46.29	46.8	46.64	45.26	46.81	46.68	46.59	45.57	45.76	46.13	45.89	46.22
TiO_2	1.35	0.96	1.8	1.16	1.65	1.56	1.54	1.86	1.42	1.56	1.61	1.24	1.35	1.55	1.76	1.72
Al_2O_3	9.69	9.62	9.4	8.78	10	9.81	9.32	10	9.56	9.17	9.6	9.84	9.74	9.18	9.49	9.34
Fe_2O_3(c)	0.17	1.12	n.d	n.d	n.d	0.76	0.72	n.d	0.79	n.d	0.27	n.d	0.32	1.2	n.d	1.01
FeO(c)	13.3	12.38	13.67	13.2	13.42	12.73	12.69	13.77	12.83	13.45	13.17	14.23	14.03	13.56	14.72	13.51
MnO	0.2	0.2	0.2	0.19	0.24	0.2	0.22	0.16	0.16	0.19	0.17	0.23	0.31	0.15	0.3	0.24
MgO	12.33	12.76	12.37	12.06	12.34	12.75	12.62	12.02	12.52	12.67	12.55	11.62	11.76	11.88	11.59	11.92
CaO	11.92	11.91	11.86	11.94	11.84	11.98	11.7	11.86	11.73	11.92	11.79	11.87	11.91	11.62	11.89	11.61
Na_2O	1.98	2	2.12	1.75	2.09	1.97	1.92	2.17	1.96	2	1.99	2.04	2.04	1.94	2.19	1.98
K_2O	0.62	0.56	0.7	0.55	0.75	0.6	0.71	0.84	0.61	0.72	0.75	0.54	0.53	0.54	0.66	0.55
F	0.01	0.1	0.04	0.04	0.13	0.05	0.04	0.04	0.08	0.11	0.08	0.05	0.03	0.02	n.d	0.09
Cl	0.03	0.02	n.d	0.03	n.d	0.01	0.01	n.d	n.d	0.01	n.d	0.01	0.02	0.02	n.d	n.d
H_2O(c)	2.02	2	2.02	1.99	2	2.05	2.03	2.02	2.02	2	2.02	1.99	2.01	2.02	2.04	2
O=F	n.d	0.04	0.02	0.02	0.05	0.02	0.02	0.01	0.03	0.04	0.03	0.02	0.01	0.01	n.d	0.04
O=Cl	0.01	n.d	n.d	0.01	n.d	n.d	n.d	n.d	n.d	n.d	n.d	n.d	n.d	n.d	n.d	n.d
Total	99.58	100.31	100.21	98.28	100.68	101.25	100.14	99.97	100.45	100.43	100.54	99.2	99.79	99.81	100.53	100.15
Si	6.777	6.811	6.759	6.939	6.749	6.766	6.818	6.678	6.817	6.822	6.792	6.768	6.758	6.8	6.751	6.786
Ti	0.149	0.105	0.198	0.13	0.181	0.169	0.169	0.206	0.155	0.171	0.176	0.139	0.15	0.172	0.195	0.19
Al/Al^{IV}	1.223	1.189	1.241	1.061	1.251	1.234	1.182	1.322	1.183	1.178	1.208	1.232	1.242	1.2	1.249	1.214
Al^{VI}	0.46	0.464	0.387	0.479	0.468	0.438	0.424	0.416	0.458	0.401	0.441	0.491	0.454	0.395	0.397	0.402
Fe^{3+}	0.018	0.123	n.d	n.d	n.d	0.082	0.079	n.d	0.086	n.d	0.029	n.d	0.036	0.133	n.d	0.111
Fe^{2+}	1.64	1.509	1.678	1.643	1.636	1.539	1.552	1.699	1.563	1.644	1.605	1.767	1.733	1.671	1.811	1.658
Mn^{2+}	0.025	0.025	0.025	0.024	0.03	0.025	0.027	0.02	0.02	0.024	0.022	0.029	0.039	0.019	0.038	0.029
Mg	2.708	2.773	2.707	2.675	2.681	2.747	2.749	2.643	2.718	2.759	2.726	2.572	2.589	2.61	2.543	2.609
Ca	1.883	1.86	1.866	1.904	1.85	1.856	1.832	1.874	1.831	1.866	1.842	1.889	1.885	1.836	1.874	1.826
Na	0.565	0.567	0.604	0.506	0.59	0.553	0.545	0.621	0.554	0.567	0.561	0.587	0.583	0.556	0.625	0.565
K	0.116	0.104	0.13	0.105	0.139	0.11	0.132	0.157	0.113	0.135	0.14	0.102	0.1	0.102	0.124	0.103
F	0.004	0.048	0.02	0.021	0.059	0.024	0.018	0.017	0.038	0.049	0.035	0.023	0.015	0.012	n.d	0.04
Cl	0.008	0.005	0.001	0.006	n.d	0.002	0.004	n.d	n.d	0.003	0.001	0.002	0.004	0.005	n.d	n.d
OH	1.988	1.948	1.979	1.972	1.941	1.974	1.979	1.983	1.962	1.949	1.964	1.976	1.981	1.984	2	1.96
Sum Cat#	17.564	17.531	17.596	17.467	17.575	17.519	17.509	17.636	17.498	17.568	17.543	17.576	17.568	17.493	17.606	17.494
X_{Mg}	0.623	0.648	0.617	0.619	0.621	0.641	0.639	0.609	0.635	0.627	0.629	0.593	0.599	0.61	0.584	0.611

n.d = not detected. (c) = calculated. c = core. r = rim.

Table 4. (Continued)

Sample Mineral	M-151-5c amphibole	M-151-6c amphibole	M-151-7c amphibole	M-178-1c amphibole	M-178-2c amphibole	M-178-3c amphibole	M-178-4c amphibole	M-178-5c amphibole	M-178-6c amphibole	M-178-7c amphibole
SiO_2	46	45.65	45.31	45.28	46.66	45.84	45.44	44.88	45.32	45.49
TiO_2	1.81	1.65	1.95	1.87	1.82	2.04	2.08	1.96	1.88	1.86
Al_2O_3	9.67	9.65	9.95	9.94	9.66	10.49	10.63	11.11	10.03	10.71
Fe_2O_3(c)	n.d	n.d	n.d	n.d	n.d	n.d	n.d	n.d	3.07	n.d
FeO(c)	14.41	14.49	14.48	13.31	12.58	13.36	12.72	13.13	10.92	13.14
MnO	0.19	0.26	0.15	0.22	0.12	0.26	0.24	0.2	0.28	0.21
MgO	11.63	11.45	11.48	12.19	12.57	12.28	12.34	11.95	12.55	12.42
CaO	12.07	12.02	11.67	11.83	12.23	12.12	12.03	12.2	11.46	12.1
Na_2O	1.93	2.13	2.21	2.04	1.84	2.03	2.15	2.12	1.99	2.06
K_2O	0.6	0.67	0.7	0.65	0.63	0.7	0.69	0.77	0.64	0.73
F	n.d	n.d	0.01	0.04	0.03	n.d	0.03	n.d	0.11	n.d
Cl	0.01	0.01	n.d	n.d	n.d	0.02	0.03	n.d	0.03	0.01
H_2O(c)	2.04	2.03	2.02	2.01	2.04	2.06	2.03	2.05	1.99	2.05
O=F	n.d	n.d	n.d	0.02	0.01	n.d	0.01	n.d	0.05	n.d
O=Cl	n.d	n.d	n.d	n.d	n.d	n.d	0.01	n.d	0.01	n.d
Total	100.35	99.98	99.92	99.37	100.16	101.21	100.38	100.36	100.21	100.79
Si	6.759	6.747	6.698	6.697	6.802	6.656	6.638	6.579	6.624	6.629
Ti	0.2	0.183	0.217	0.208	0.199	0.223	0.228	0.216	0.206	0.204
Al/Al^{IV}	1.241	1.253	1.302	1.303	1.198	1.344	1.362	1.421	1.376	1.371
Al^{VI}	0.433	0.428	0.431	0.429	0.462	0.451	0.469	0.498	0.352	0.469
Fe^{3+}	n.d	n.d	n.d	n.d	n.d	n.d	n.d	n.d	0.337	n.d
Fe^{2+}	1.77	1.791	1.79	1.646	1.533	1.623	1.554	1.609	1.334	1.602
Mn^{2+}	0.023	0.032	0.019	0.028	0.015	0.032	0.03	0.024	0.035	0.025
Mg	2.546	2.522	2.53	2.688	2.732	2.658	2.686	2.611	2.735	2.698
Ca	1.9	1.904	1.849	1.875	1.91	1.885	1.883	1.916	1.795	1.89
Na	0.551	0.61	0.632	0.585	0.519	0.572	0.608	0.602	0.564	0.583
K	0.113	0.126	0.132	0.123	0.117	0.13	0.129	0.144	0.119	0.136
F	n.d	n.d	0.004	0.017	0.016	n.d	0.015	n.d	0.053	n.d
Cl	0.002	0.002	n.d	n.d	n.d	0.004	0.007	n.d	0.007	0.002
OH	1.998	1.998	1.996	1.983	1.984	1.996	1.978	2	1.94	1.997
Sum Cat#	17.537	17.596	17.6	17.583	17.487	17.574	17.587	17.619	17.478	17.606
X_{Mg}	0.59	0.585	0.586	0.62	0.64	0.621	0.634	0.619	0.672	0.627

Table 5. Amphibole analyses from the dolerite dykes crosscutting the metamorphic sole rocks of the Mersin ophiolite.

Sample	M-77-1c	M-77-2c	M-77-3c	M-77-4c	M-77-4r	M-77-5c	M-77-6c	M-77-7c	M-77-8c	M-77-9c	M-77-10c	M-77-11c	M-77-12c	M-77-13c	M-77-14c
SiO_2	55.91	46.01	45.07	44.74	47.56	45.15	48.53	44.64	47.2	46.64	47.94	47.61	49.04	47.21	45.87
TiO_2	0.09	1.05	1.28	1.4	0.67	1.35	0.62	1.42	0.78	1.33	0.89	0.59	0.78	0.95	1.1
Al_2O_3	1.75	8.32	8.54	8.89	6.24	8.24	6.88	8.76	7	7.89	6.82	7.21	6.45	7.6	8.17
Fe_2O_3(c)	n.d	12.05	12.23	12.22	7.5	10.51	10.92	10.06	11.29	6.57	8.33	11.58	9.29	9.89	10.18
FeO(c)	11.52	11.95	12.96	13.12	15.17	14.27	10.65	14.22	10.27	12.92	11.48	9.59	9.2	10.41	12.53
MnO	0.22	0.38	0.46	0.39	0.58	0.37	0.43	0.33	0.24	0.36	0.34	0.33	0.37	0.35	0.43
MgO	16.5	8.7	7.79	7.36	9.01	7.5	10.42	7.61	10.2	10.33	10.83	10.68	12.08	10.95	8.64
CaO	13.06	10.26	10.02	9.78	10.62	10	10.52	10.35	10.23	11.21	10.89	10.36	10.87	10.93	10.17
Na_2O	0.2	1.19	1.4	1.37	1.27	1.39	0.9	1.26	0.98	1.21	0.99	1.06	0.82	1.13	1.23
K_2O	0.03	0.06	0.06	0.07	0.42	0.07	0.04	0.06	0.04	0.07	0.05	0.07	0.06	0.04	0.05
F	n.d	0.03	n.d	n.d	n.d	n.d	n.d	n.d	0.01	n.d	n.d	0.01	n.d	0.01	0.01
Cl	n.d	0.09	0.1	0.08	0.04	0.08	0.06	0.08	0.03	0.07	0.07	0.07	0.03	0.05	0.1
H_2O(c)	2.13	2.02	2.01	2	2.01	1.99	2.06	1.99	2.03	2.02	2.03	2.04	2.07	2.05	1.99
O=F	n.d	0.01	n.d	n.d	n.d	n.d	n.d	n.d	0.01	n.d	n.d	n.d	n.d	n.d	n.d
O=Cl	n.d	0.02	0.02	0.02	0.01	0.02	0.01	0.02	0.01	0.02	0.01	0.02	0.01	0.01	0.02
Total	101.41	102.08	101.91	101.4	101.08	100.89	102.02	100.78	100.29	100.6	100.65	101.18	101.08	101.56	100.44
Si	7.857	6.724	6.647	6.63	7.052	6.731	7	6.661	6.931	6.86	7.007	6.917	7.064	6.846	6.799
Ti	0.01	0.115	0.142	0.156	0.074	0.151	0.067	0.16	0.086	0.147	0.098	0.064	0.085	0.104	0.123
Al/Al^{IV}	0.143	1.276	1.353	1.37	0.948	1.269	1	1.339	1.069	1.14	0.993	1.083	0.936	1.154	1.201
Al^{VI}	0.147	0.158	0.132	0.183	0.142	0.178	0.169	0.202	0.143	0.228	0.181	0.151	0.16	0.146	0.226
Fe^{3+}	n.d	1.325	1.357	1.363	0.837	1.179	1.185	1.13	1.247	0.727	0.916	1.266	1.007	1.079	1.135
Fe^{2+}	1.354	1.461	1.599	1.626	1.881	1.779	1.285	1.774	1.262	1.59	1.404	1.165	1.108	1.262	1.553
Mn^{2+}	0.027	0.047	0.058	0.049	0.073	0.046	0.053	0.042	0.03	0.044	0.042	0.041	0.045	0.043	0.054
Mg	3.456	1.894	1.712	1.625	1.992	1.666	2.241	1.693	2.232	2.264	2.359	2.314	2.595	2.366	1.909
Ca	1.966	1.607	1.584	1.553	1.687	1.597	1.626	1.655	1.61	1.766	1.706	1.613	1.678	1.698	1.616
Na	0.054	0.337	0.401	0.394	0.366	0.403	0.251	0.366	0.28	0.346	0.279	0.3	0.23	0.318	0.355
K	0.005	0.012	0.011	0.013	0.079	0.012	0.008	0.012	0.007	0.013	0.009	0.012	0.012	0.007	0.009
F	n.d	0.012	n.d	n.d	n.d	n.d	n.d	n.d	0.006	n.d	n.d	0.005	n.d	0.003	0.004
Cl	n.d	0.023	0.026	0.021	0.01	0.02	0.015	0.02	0.007	0.017	0.016	0.017	0.007	0.012	0.026
OH	1.999	1.965	1.974	1.979	1.99	1.979	1.984	1.98	1.987	1.983	1.983	1.979	1.993	1.985	1.97
Sum Cat#	17.018	16.956	16.995	16.96	17.132	17.012	16.885	17.033	16.897	17.124	16.994	16.925	16.92	17.023	16.979
X_{Mg}	0.719	0.565	0.517	0.5	0.514	0.484	0.636	0.488	0.639	0.588	0.627	0.665	0.701	0.652	0.551

n.d = not detected. (c) = calculated. c = core. r = rim.

Table 6. Pyroxene analyses from the metamorphic sole rocks and crosscutting dolerite dykes of the Mersin ophiolite.

Sample Rock Type	M-77-3 dolerite	M-77-4 dolerite	M-178-1 amphibolite	M-178-2 amphibolite	M-178-3 amphibolite	M-178-4 amphibolite	M-178-5 amphibolite	M-178-6 amphibolite	M-178-7 amphibolite
SiO_2	52.8	52.89	52.42	52.11	51.9	52.6	52.87	52.89	53.03
TiO_2	0.37	0.31	0.24	0.29	0.24	0.27	0.25	0.24	0.27
Al_2O_3	2.17	2.1	2.16	2.16	2.01	2.34	2.13	2.2	2.21
Cr_2O_3	0.08	0.12	0.03	0.08	0.06	0.12	0.1	0.08	0.16
Fe_2O_3(c)	0.66	n.d	0.74	0.25	1.18	0.16	n.d	n.d	n.d
FeO(c)	6.96	7.51	7.75	8.05	7.19	8.17	8.2	8.18	8.23
MnO	0.19	0.23	0.3	0.26	0.29	0.29	0.31	0.31	0.27
MgO	16.64	16.67	13.16	12.85	12.97	12.87	13.06	12.97	12.78
CaO	20.1	19.69	22.2	22.3	22.44	22.42	22.47	22.41	22.5
Na_2O	0.19	0.16	0.64	0.6	0.63	0.65	0.61	0.63	0.64
Total	100.16	99.67	99.64	98.96	98.9	99.9	100	99.9	100.1
Si	1.939	1.951	1.958	1.961	1.954	1.960	1.967	1.969	1.971
Ti	0.01	0.009	0.007	0.008	0.007	0.008	0.007	0.007	0.007
Al/Al^{IV}	0.061	0.049	0.042	0.039	0.046	0.04	0.033	0.031	0.029
Al^{VI}	0.033	0.042	0.053	0.057	0.043	0.063	0.061	0.066	0.068
Cr	0.002	0.003	0.001	0.002	0.002	0.004	0.003	0.002	0.005
Fe^{3+}	0.018	n.d	0.021	0.007	0.033	0.005	n.d	n.d	n.d
Fe^{2+}	0.214	0.232	0.242	0.253	0.226	0.255	0.255	0.255	0.256
Mn^{2+}	0.006	0.007	0.009	0.008	0.009	0.009	0.01	0.01	0.009
Mg	0.911	0.916	0.733	0.721	0.728	0.715	0.724	0.72	0.708
Ca	0.791	0.778	0.888	0.899	0.905	0.895	0.896	0.894	0.896
Na	0.014	0.011	0.046	0.044	0.046	0.047	0.044	0.045	0.046
Sum Cat#	4.000	3.999	4.000	4.000	4.000	4.000	4.000	3.998	3.994
Wo(Ca)	41.283	40.407	47.685	48.002	48.688	48.000	47.764	47.842	48.182
En(Mg)	47.559	47.572	39.325	38.471	39.144	38.342	38.627	38.532	38.059
Fs(Fe^{2+})	11.159	12.021	12.989	13.528	12.168	13.658	13.609	13.626	13.759
X_{Mg}	0.81	0.798	0.752	0.74	0.763	0.737	0.739	0.739	0.734

n.d = not detected. (c) = calculated.

an albite (An_{2-4}) composition. However, plagioclase with andesine and labradorite compositions was commonly observed in amphibolites from the other metamorphic sole rocks of the Tauride Belt Ophiolites (Çelik 2002; Çelik & Delaloye 2006). Epidote, abundant in the upper part of the metamorphic sole rocks, occurs as both a primary and secondary mineral in the amphibolites and is especially abundant in veinlets.

The lower part of the metamorphic sole rocks is composed mainly of quartz-feldspar-mica schist, amphibole-quartz-feldspar-mica schist, quartz-mica schist and quartzite. The most common texture of the mica schists is granolepidoblastic. The mineral assemblages in the metamorphic sole rocks and their dolerite dykes are given in Table 2.

Dolerite dykes cutting the metamorphic sole rocks consist of amphibole, pyroxene, plagioclase, secondary minerals (e.g., epidote, quartz, chlorite), and accessory minerals (titanite and ilmenite). The dykes show subophitic and microgranular textures. Some of the dykes have been extensively affected by hydrothermal alteration. While quartz is a minor constituent of the dolerite dykes, amphibole is abundant: ferro-hornblende, magnesio-hornblende and actinolite were all observed. Plagioclases exhibit alteration minerals such as kaolinite and epidote but fresh plagioclases in the same rocks are also observed,

Table 7. Feldspar analyses from the amphibolites of the metamorphic sole rocks of the Mersin ophiolite.

Sample	M154-1	M154-2	M154-3	M154-4	M154-5	M154-6c	M154-6r1	M154-6r2	M154-7c	M154-8c	M154-9c	M154-10c	M154-11c	M154-12c
SiO_2	66,45	66,53	69,6	68,17	68,69	69,21	69,35	67,88	68,75	66,29	67,9	66,78	68,11	69,35
Al_2O_3	19,85	20,23	20,04	19,7	20,14	19,99	19,9	19,95	20,06	20,44	20,47	20,17	20,19	20,24
Fe_2O_3	n.d	0,05	n.d	0,08	0,1	0,04	n.d	0,02	0,01	0,05	0,02	n.d	0,04	0,02
MgO	0,01	0,01	n.d	n.d	n.d	n.d	n.d	n.d	0,01	n.d	n.d	0,01	n.d	0,05
CaO	0,69	0,82	0,75	0,74	0,75	0,63	0,67	0,74	0,77	0,92	1,01	0,84	0,78	0,98
BaO	n.d	n.d	n.d	n.d	n.d	n.d	n.d	n.d	n.d	n.d	n.d	n.d	n.d	0,03
Na_2O	11,35	11,37	11,23	11,11	11,37	11,44	11,49	11,2	11,34	11,27	11,07	11,31	11,38	11,09
K_2O	0,1	0,1	0,11	0,1	0,12	0,07	0,09	0,1	0,1	0,09	0,09	0,09	0,1	0,1
Total	98,45	99,11	101,73	99,9	101,18	101,38	101,51	99,88	101,04	99,05	100,56	99,21	100,6	101,87
Si	2,99	2,977	2,987	2,982	2,97	2,983	2,986	2,971	2,975	2,969	2,987	2,983	2,996	2,975
Al/Al^{IV}	1,007	1,021	1,014	1,016	1,026	1,015	1,01	1,029	1,023	1,032	1,016	1,016	1,003	1,023
Al^{VI}	n.d	n.d	n.d	n.d	n.d	n.d	n.d	n.d	n.d	n.d	n.d	n.d	n.d	n.d
Fe^{3+}	n.d	0,002	n.d	0,003	0,003	0,001	n.d	0,001	n.d	0,002	0,001	n.d	0,001	0,001
Mg	0,001	0,001	n.d	n.d	n.d	n.d	n.d	n.d	0,001	n.d	n.d	0,001	n.d	0,003
Ca	0,032	0,038	0,034	0,035	0,035	0,029	0,031	0,035	0,036	0,042	0,046	0,039	0,035	0,045
Na	0,947	0,944	0,935	0,942	0,954	0,956	0,959	0,95	0,951	0,936	0,904	0,937	0,929	0,923
K	0,005	0,005	0,006	0,005	0,007	0,004	0,005	0,005	0,006	0,005	0,005	0,005	0,005	0,006
Sum Cat#	4,982	4,987	4,976	4,983	4,995	4,989	4,991	4,992	4,992	4,985	4,959	4,98	4,97	4,977
Ab	96,235	95,633	95,85	95,92	95,845	96,668	96,386	95,937	95,84	95,233	94,729	95,533	95,816	94,739
An	3,227	3,827	3,518	3,523	3,493	2,93	3,101	3,524	3,579	4,275	4,78	3,942	3,614	4,634
Or	0,537	0,539	0,632	0,557	0,661	0,401	0,513	0,539	0,581	0,492	0,49	0,525	0,565	0,583

n.d = not detected. c = core. r = rim.

Table 8. K-Ar ages and analytical data for the amphibolite and dolerite dykes from the Mersin ophiolite.

Sample	Rock	Mineral	% K	$^{40}Ar^*$ moles/g × 10^{-11}	% $^{40}Ar^*$	$^{40}Ar/^{36}Ar \times 10^2$	$^{40}K/^{36}Ar \times 10^4$	Age	in	Ma
M-175	amphibolite	hornblende	0.50	8.294	96.0	73.26	125.75	93.8	±	3
M-82	dolerite dyke	whole rock	0.97	14.537	91.2	33.58	60.99	84.4	±	3
M-87	dolerite dyke	whole rock	1.30	20.514	89.6	28.49	48.30	88.8	±	2

indicating recrystallization during the hydrothermal alteration phase. Some pyroxenes in the dolerite dykes occur as relict grains surrounded by reaction rims of green-brown to green hornblende. Pyroxene is more abundant in dykes over 30 cm thick. Pyroxenes from the dolerite dyke sample M-77 are augite in composition. Ilmenite is generally observed as dendritic crystals in pyroxene-rich dolerite dykes. The dykes range from 10 cm to 5–6 m thick and some exhibit well-developed chilled margins.

Geochemistry

Cr values of the amphibolites in the Mersin ophiolite range from 55 ppm to 1292 ppm. All the amphibolites are of igneous origin, based on the Cr-TiO_2 diagram of Leake (Leake 1964) (Figure 2a), and are probably derived from mafic rocks such as basalts and gabbros. The mica schists were derived from sedimentary and volcano-sedimentary rocks, as are other mica schists from the metamorphic sole rocks of the Lycian and Pozantı-Karsantı ophiolites (Çelik 2007). On a $Na_2O + 31/47K_2O - Al_2O_3$ diagram (Fonteilles 1976), the mica schists plot in the fields of lithic sandstone and greywacke protoliths (Figure 2b).

In the SSZ systems, three different end-member components can be considered to melt to form MORB, OIB and IAT basalt compositions and variable mixing between these three end-member components may form lava compositions between MORB-OIB and MORB-IAT (Leat *et al*. 2000, 2004). On a TiO_2-MnO-P_2O_5 diagram (Mullen 1983), amphibolites plot in the ocean island alkali and tholeiite (OIA, OIT) and island arc tholeiite (IAT) basalt fields, whereas the dolerite dykes plot mostly in the IAT field (Figure 3a). The arc signature of the dyke samples is shown on a Ti-V diagram (Figure 3b), where the amphibolites are represented by OIB, excluding two amphibolites and one dolerite sample that exhibit a MORB signature. On a TiO_2-Zr diagram, amphibolites from the metamorphic sole rocks of the Mersin and other Tauride Belt ophiolites exhibit SSZ geochemical charactersitics, with IAT, MORB, and OIB-like affinities and probable mixing of these end-members (Figure 4a). On the same diagram, dolerite dykes from the Mersin ophiolite clearly exhibit an arc-related origin, as do other dolerite dykes from the other Tauride Belt ophiolites. According to the Cr-Y diagram, all the dolerite dykes and one amphibolite sample (M-157) from the metamorphic sole rocks of the Mersin ophiolite plot in the IAT field, indicating subduction influence during their generation (Figure 4b). The dolerite dykes and the metamorphic sole rocks of the Tauride Belt Ophiolites thus have very similar geochemical characteristics to the volcanic rocks of the active back-arc spreading centre (East Scotia Ridge) located to the west of the South Sandwich island arc, based on the Cr-Y and TiO_2-Zr diagrams. The REE patterns of the amphibolites from the Mersin ophiolite exhibit two different groups (Figure 5a). The first is characterized by LREE enrichment typical of WPB (or seamount). In this group, the La_N/Yb_N ratio of one amphibolite sample (M-78) is 2.05. This sample should be interpreted as N-MORB or a transition rock from N-MORB to enriched MORB (E-MORB). The second group of amphibolites, including the dolerite dykes, exhibits a relatively flat pattern. Slight depletion in LREE could be interpreted by derivation from a MORB source. However, La_N/Yb_N ratios (0.56–1.29) of the dolerite dykes (except M-86) and the amphibolites from the second group are similar to the La_N/Yb_N ratios (0.63–1.45) of the dolerite dykes from the Lycian ophiolites, which are located further west than the Mersin ophiolite. Lead isotope compositions of the dolerite dykes from the Lycian ophiolites indicate a subduction-related origin and exclude their derivation solely from a MORB source (Çelik & Chiaradia 2008). The crystallization age of the dolerite dykes of the Mersin and the Lycian ophiolites is also similar (Çelik *et al*. 2006). All these data indicate that the dolerite dykes of the Mersin ophiolite were formed in a subduction-related environment. On the N-MORB normalized spider diagram, the first group of amphibolites exhibits multi-element patterns more enriched than N-MORB (Figure 5b) and similar to OIB basalts. The second group of amphibolites displays slight enrichment in large ion lithophile elements (LILE; Rb, Th) compared to Nb and REE. Their compositions, however, are similar to N-MORB or

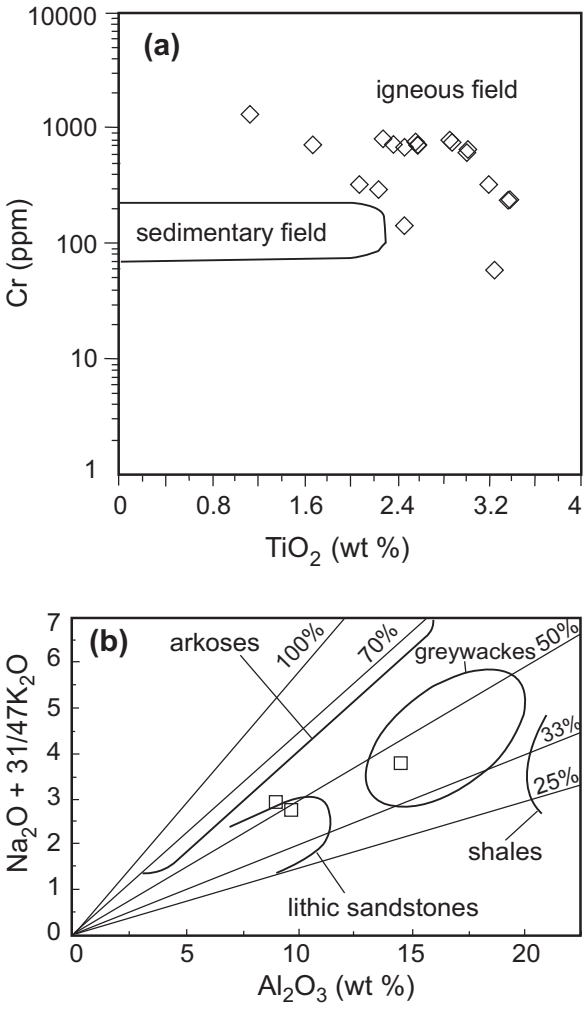

Figure 2. (a) Cr versus TiO_2 for the amphibolites. Outside the ringed area represents igneous protoliths; (b) alkalis versus Al_2O_3 diagram showing the original sedimentary lithologies of the mica schists from the metamorphic sole rocks of the Mersin ophiolite.

transitional between N-MORB and E-MORB. The dolerite dykes exhibit LILE enrichment (K, Rb, Sr, Ba) relative to some high-field-strength elements (HFSE) such as Nb, Zr, Ti (Figure 5c), suggesting that they were formed as IAT-like dolerites in a subduction related environment. However, LILE are strongly affected by alteration and metamorphic processes, therefore characterization and discrimination of metamorphic and magmatic suites has been done using trace elements generally considered relatively stable (immobile) during alteration, such as HFSE and REE (Beccaluva 1979; Pearce 1982; Thompson 1991). All the dolerite dykes have small negative Eu

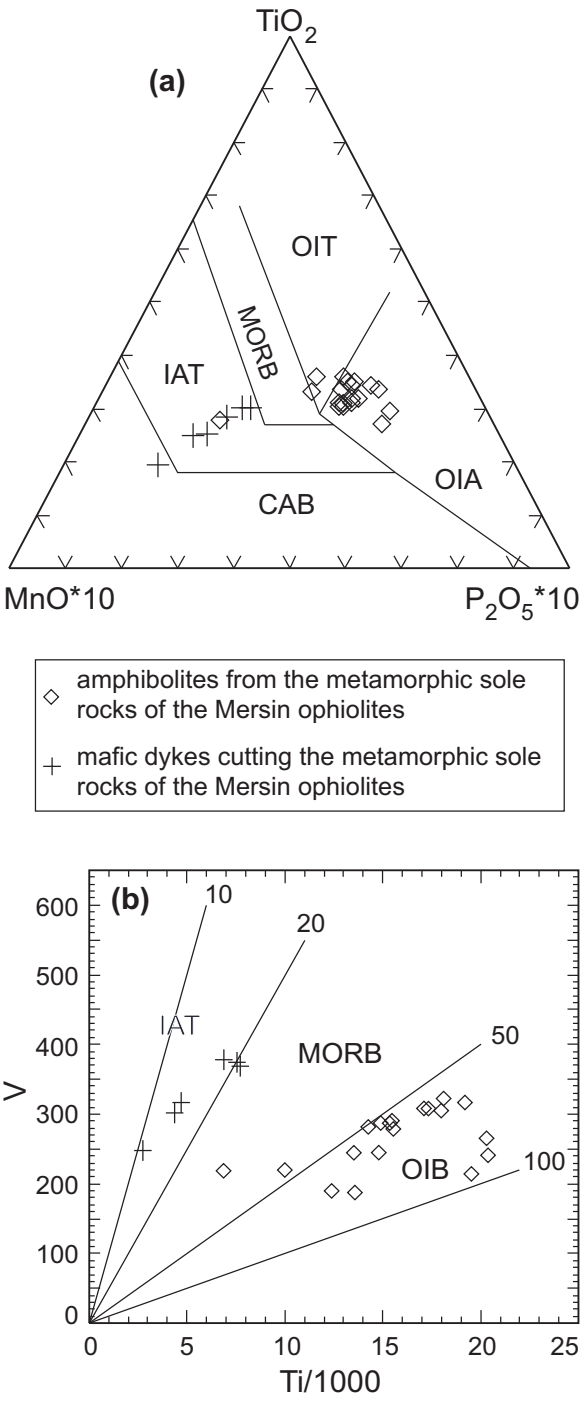

Figure 3. (a) TiO_2-MnO-P_2O_5 discrimination diagram (Mullen 1983) for the amphibolites and the dolerite dykes in the metamorphic sole rocks of the Mersin ophiolite; (b) Ti versus V diagram showing tectonomagmatic environment of dolerite and amphibolite rocks in the metamorphic sole rocks of the Mersin ophiolite, after Shervais (1982).

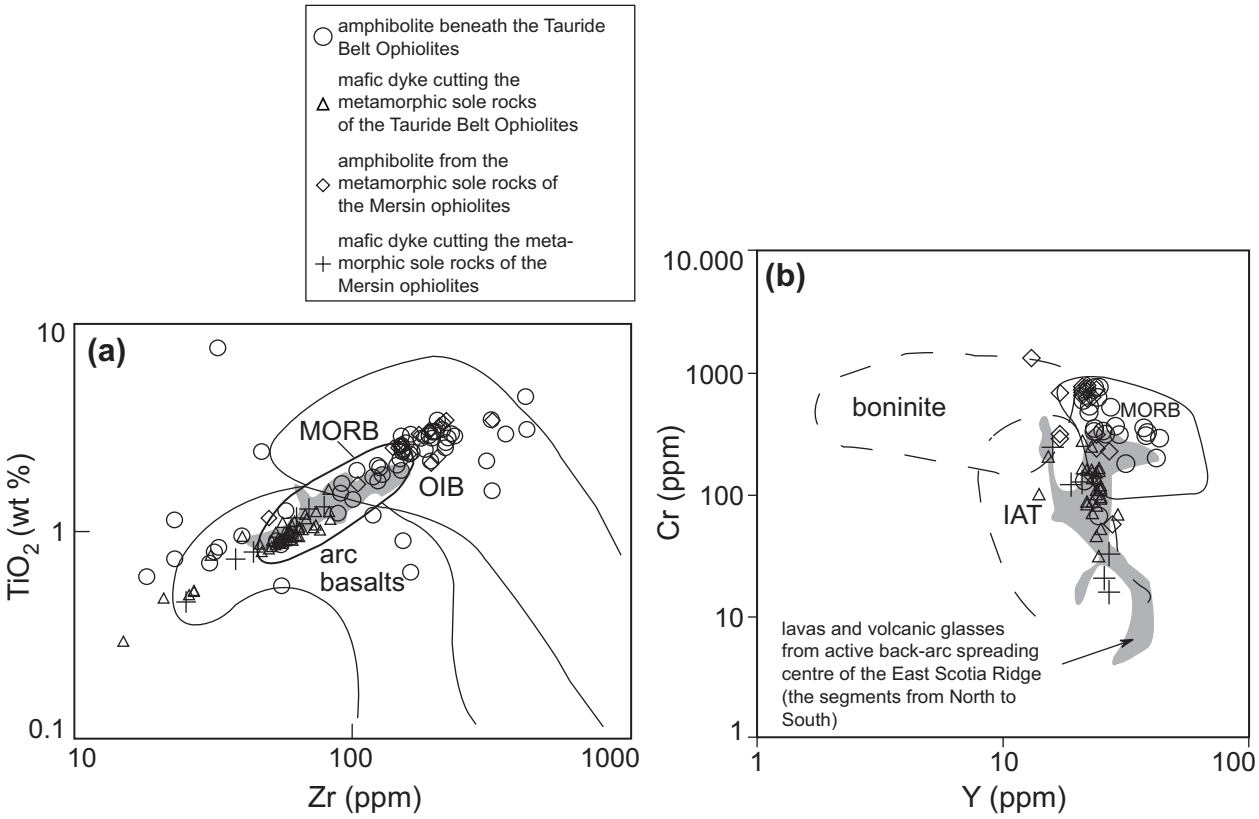

Figure 4. (a) TiO_2 versus Zr tectonomagmatic discrimination diagram for the metamorphic sole rocks and their crosscutting mafic dykes from the Tauride Belt ophiolites and the East Scotia Ridge rock samples (shaded) from the South Sandwich arc-basin system. Fields for MORB, IAT and OIB after Pearce (1980); (b) Cr-Y plot after Pearce *et al.* (1981), showing fields for boninite, IAT, and MORB. Data for the East Scotia Ridge are from Fretzdorff *et al.* (2002) and Leat *et al.* (2004). Data for the amphibolites and mafic dykes from the Tauride Belt Ophiolites are from Lytwyn & Casey (1995), Polat & Casey (1996), Dilek *et al.* (1999), Çelik & Delaloye (2003, 2006), Çelik (2007).

anomalies (Eu/Eu* = 0.98–0.87) suggesting plagioclase fractionation in their origin. However, the amphibolites exhibit both small negative (0.98–0.87) and positive (1.13–1.09) Eu anamolies. The latter values should be consistent with plagioclase accumulation in their protoliths.

The Sm/Yb-Ce/Sm ratio was used to characterize mantle source regions for the amphibolites and mafic dykes (Figure 6a). The high Sm/Yb and Ce/Sm ratios of the amphibolites beneath the Mersin ophiolite and in the mafic dykes (pyroxenite and dolerite) cutting the amphibolites of the other Tauride Belt ophiolites suggest that they were derived from melting of OIB-like enriched mantle source, whereas the dolerite dykes and some of the amphibolites with low Sm/Yb and Ce/Sm ratios plot in the field of tholeiitic amphibolites from the Tauride Belt ophiolites.

Nb depletion and Th enrichment in volcanic rocks is typical of a subduction influence (Saunders & Tarney 1979, 1984; Pearce *et al.* 1984). Moreover, Th is a key element in subduction zone discrimination and is enriched in all arc lavas, and so is mobilized in subduction zones, but it is immobile until the temperature approaches the melting temperature (Johnson & Plank 1999; Pearce 2003). Nb/Nd versus Th/Nb ratios were used to show the mantle source regions and the subduction influence for the amphibolites and mafic dykes (Figure 6b). Th/Nb ratios of the most of the amphibolites and mafic dykes are higher than the average N-MORB and OIB values, suggesting that the subduction influence was common during the generation of the mafic dykes and the protoliths of the amphibolites.

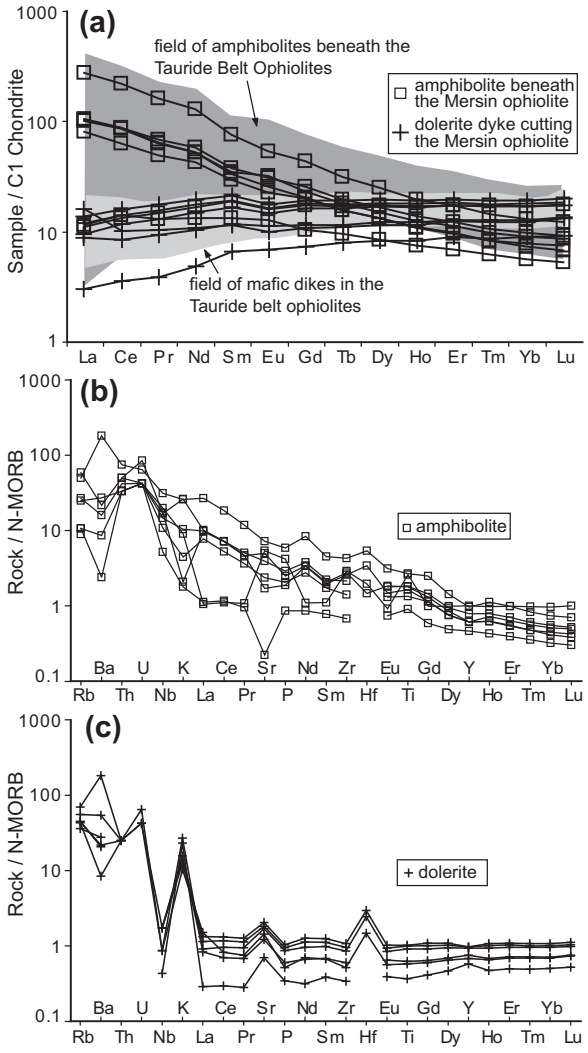

Figure 5. (a) Chondrite-normalized REE plots for amphibolites and dyke rocks from the metamorphic sole rocks of the Mersin ophiolite. Normalizing values are from Sun & McDonough (1989). Data for the amphibolites and mafic dykes from the Tauride Belt Ophiolites are from Dilek *et al.* (1999), Çelik & Delaloye (2003, 2006), Çelik (2007); (b, c) MORB–normalized trace element patterns of the amphibolites and cross-cutting dolerite dykes from the metamorphic sole rocks of the Mersin ophiolite.

Thermobarometrical and Geochronological Investigations

The amphibolites from the metamorphic sole rocks have restricted mineral assemblages (e.g., hornblende and plagioclase) and provide only limited information about their metamorphic conditions.

The Na content in the M4 site of amphibole may be a useful semi-quantitative geobarometer for amphibolites formed in amphibolite and greenschist facies (Brown 1977; Laird *et al.* 1984). The pressure for the metamorphic sole rocks, deduced from the proportions of Na^{M4}-Al^{IV} and Al^{VI}-Si numbers of amphiboles, is less than 5 kb (Figure 7a, b). These pressure estimates are in agreement with the compositions of all analysed amphiboles that plot in the low-pressure (*LP*) to medium-pressure (*MP*) domain of Laird *et al.* (1984) (Figure 7c). Similar pressure values were also obtained from the metamorphic sole rocks of the Beyşehir and Pozantı-Karsantı ophiolites (Çelik & Delaloye 2006; Çelik 2007). Temperature conditions at the time of metamorphism for the metamorphic sole rocks were calculated using the hornblende-plagioclase thermometer of Holland & Blundy (1994). Sample M-154 consists of hornblende, plagioclase, sphene and opaque minerals. Since quartz is absent from the assemblage, the edenite-richterite thermometer was used on the formula. The calculated temperature is 522 ± 15 °C within a 1σ confidence interval.

K-Ar ages may be unreliable, due to mobility of Ar and/or excess Ar, and should be treated with caution. The effects of excess Ar and of alteration can be minimized using the $^{40}Ar/^{39}Ar$ method. Therefore, K-Ar ages were compared with more reliable $^{40}Ar/^{39}Ar$ ages in order to explore their geochronological reliability. K-Ar age determination on hornblende from sample M-175 (amphibolite) yielded 93.8 ± 3 Ma (2σ) (Table 8). Dilek *et al.* (1999) presented ^{40}Ar-^{39}Ar plateau ages of 91.3 ± 0.4 and 93.8 ± 0.5 Ma for two amphibolites from Mersin ophiolite, which they interpreted as cooling ages. Parlak *et al.* (1995) presented a K-Ar age of 93.4 ± 2 Ma for amphibolites from the Mersin ophiolite. Parlak & Delaloye (1999) calculated a weighted mean ^{40}Ar-^{39}Ar age of amphibolites (hornblende) of 92.6 ± 0.2 Ma and interpreted this as the age of the intra-oceanic thrusting, during which sub-ophiolitic metamorphic sole rocks were developed. Thus the K-Ar age data (93.8 ± 3 Ma) in this study agrees with previously obtained ^{40}Ar-^{39}Ar age data (Dilek *et al.* 1999; Parlak & Delaloye 1999). However, closure temperature of amphibole in the ^{40}Ar-^{39}Ar system was estimated to be approximately 500–550 °C for moderate cooling rates (Harrison 1981), and hence the metamorphic temperature in the sole rocks, calculated as 522 ± 15 °C, corresponds to the closure temperature of amphibole in ^{40}Ar-^{39}Ar system. Therefore ~ 91–93 Ma

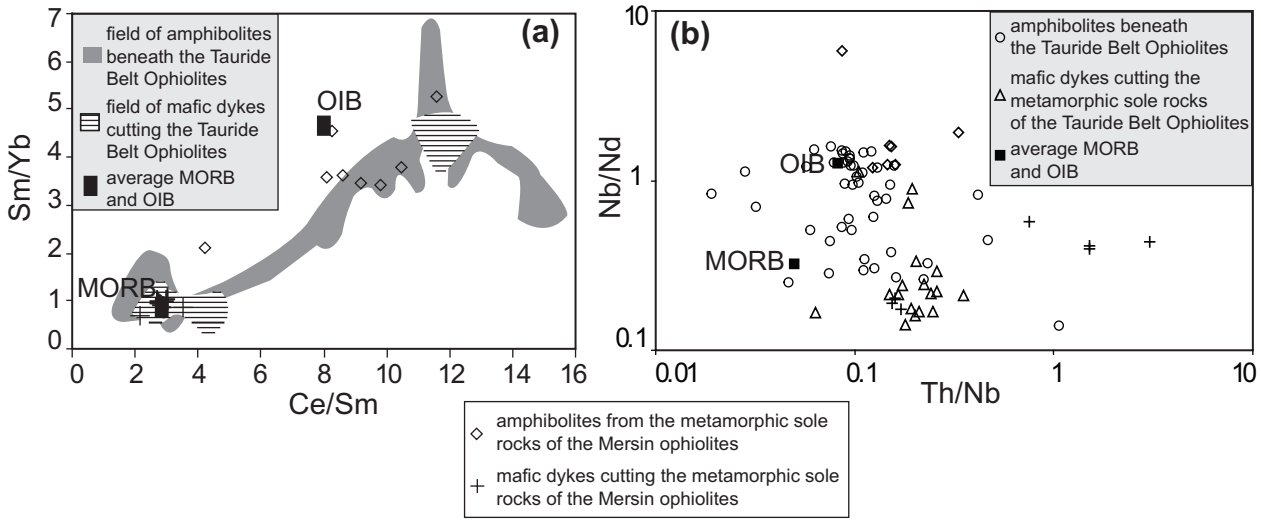

Figure 6. (a) Sm/Yb versus Ce/Sm diagram, after Pearce (1982), showing source characteristics for the dolerite dykes and the amphibolites. Fields of OIB and MORB are from Sun & McDonough (1989). Data for the metamorphic soles and mafic dykes from the Tauride Belt Ophiolites are from Lytwyn & Casey (1995), Parlak *et al.* (1995), Polat & Casey (1996), Dilek *et al.* (1999), Çelik & Delaloye (2003, 2006), Çelik (2007); Çelik & Chiaradia (2008). (b) Nb/Nd versus Th/Nb diagram showing source characteristics and subduction influence for the amphibolites and the dolerite dykes of the metamorphic sole rocks from the Tauride Belt Ophiolites. Fields of OIB and MORB are from Sun & McDonough (1989). Data for the metamorphic sole rocks and dolerite dykes from the Tauride Belt ophiolites are from Polat & Casey (1996), Dilek *et al.* (1999), Çelik & Delaloye (2003, 2006), Çelik (2007), Çelik & Chiaradia (2008).

could also be interpreted as the approximate metamorphic age of the amphibolites.

Dilek *et al.* (1999) obtained $^{40}Ar/^{39}Ar$ ages of 91.0 ± 0.6 Ma from one dolerite dyke from the Mersin ophiolite. Parlak & Delaloye (1996) also dated dolerite dykes (as whole rock analyses) from the Mersin Ophiolite using the $^{40}Ar/^{39}Ar$ method. They obtained ages ranging from 63.8 ± 0.9 to 89.6 ± 0.7 Ma and interpreted these ages as crystallization ages indicating the time of the dyke emplacement. Koepke *et al.* (2002) reported that both the age and remarkable similarity in composition and structure of the ophiolites of Karpathos and Rhodes (southern Aegean islands) to ophiolite occurrences in southern Turkey demonstrates that they also belong to the Cretaceous ophiolite belt of the Taurides. They obtained K-Ar ages from dolerite dykes ranging from 74.5 ± 2.2 to 95.3 ± 4.2 Ma, with a mean age around 87 Ma. In this study, K-Ar age determinations on the dolerite dykes cutting the metamorphic sole rocks yield ages between 88.8 ± 2 and 84.4 ± 3 Ma (Table 8). As mentioned before, dolerite dykes in the Mersin ophiolite do not cut the mélange and platform carbonates. While some of the dykes have chilled margins, others do not. All of these data from the dolerite dykes suggest that dyke injections into the metamorphic sole rocks of the Mersin ophiolite were common at different times after the generation of the metamorphic sole rocks, but predated the emplacement of the Mersin ophiolite on to the Tauride platform carbonates.

Discussion and Conclusion

The Western Pacific is a natural laboratory for investigating subduction models and their link to ophiolites. Cenozoic SSZ systems of the Western Pacific basins include mature and immature SSZ systems, such as Tonga-Kermadec, Mariana-Izu-Bonin and Lau. Backarc basin crust forms at spreading centres that in many backarc basins, erupt tholeiitic melts with mineral and chemical signatures ranging from N-MORB to IAT (Hawkins & Melchior 1985; Gribble *et al.* 1988, 1996; Hawkins 1995a, b). Seamounts in the backarc basins range in composition from island arc chemistry to OIB (Hawkins 2003). The Lau and Mariana Trough backarc basins contain a wide range of rock compositions with N-MORB, IAT, BABB and enriched basalts including OIB, as well as fractionated rocks of these series (Hawkins 2003). One source of SSZ magmas is mantle material convectively entrained above a subduction

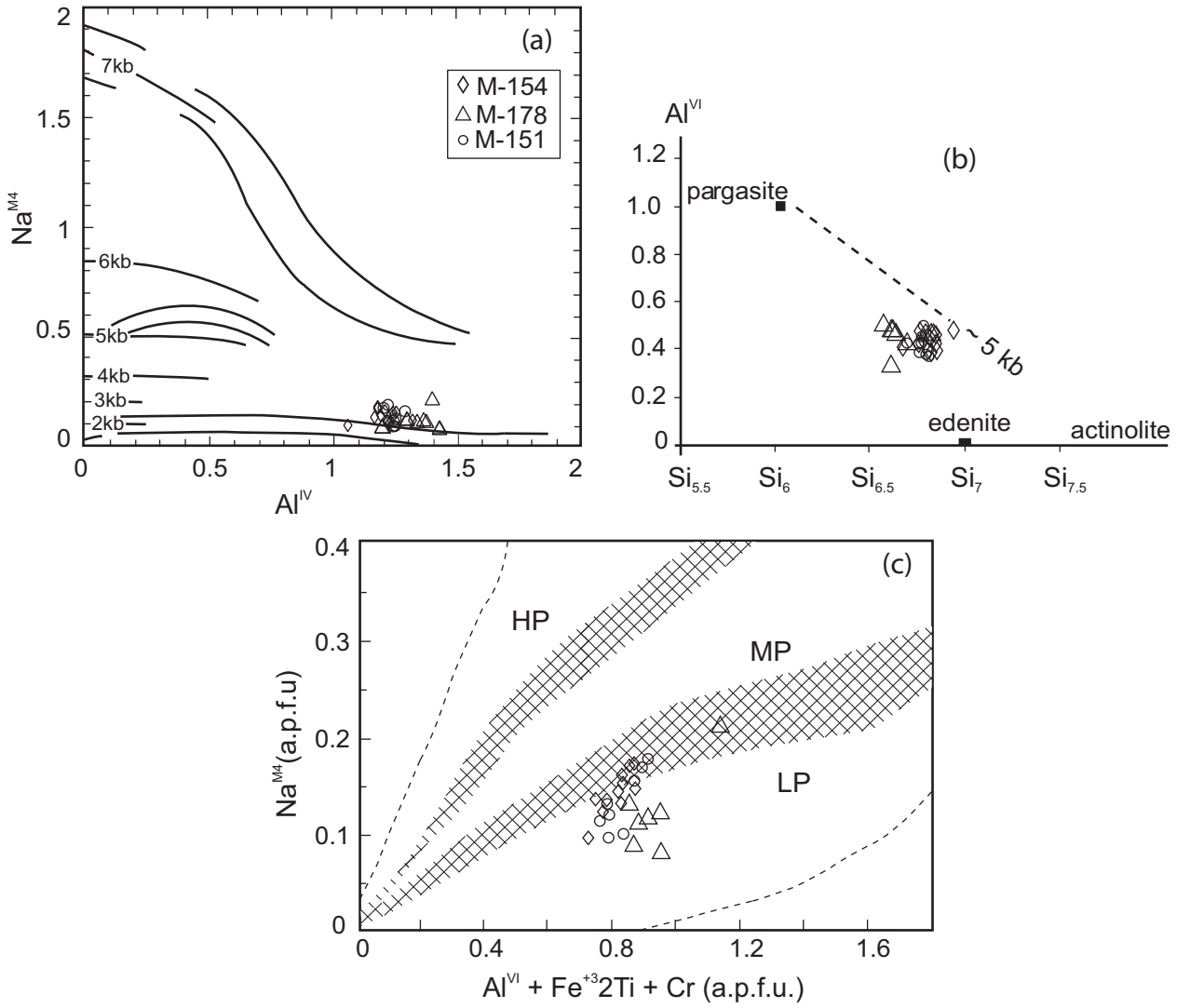

Figure 7. (a) Comparison of Na^{M4} and Al^{IV} for amphibole from amphibolites of the metamorphic sole rocks, after Brown (1977); (b) Al^{VI} versus Si diagram (Raase 1974) for amphiboles in the amphibolites; (c) Amphiboles from the metamorphic sole rocks of the Mersin ophiolite plotted in the pressure discrimination diagram of Laird *et al.* (1984).

zone by viscous drag exerted by the subducted plate, and brought in under the backarc basin (Ewart & Hawkesworth 1987). This 'new' mantle may be relatively fertile and capable of generating N-MORB, E-MORB, or OIB (Hawkins 1976, 1995a, b; Ikeda & Yuasa 1989; Hawkins *et al.* 1990; Volpe *et al.* 1990).

As indicated in the geochemistry section, the amphibolites of the metamorphic sole rocks from Tauride Belt Ophiolites, including the Mersin ophiolite, are generally metamorphosed equivalents of IAT-, MORB-, E-MORB- and OIB-type basaltic rocks. Petrographic and geochemical results of ophiolite-related intrusives and extrusives suggest that the Late Cretaceous ophiolites of the Tauride belt were formed in a SSZ environment (Pearce *et al.* 1984; Parlak *et al.* 1996, 2002; Çelik *et al.* 2006) (Figure 8a, b). Protoliths of the IAT-, OIB- and MORB-like amphibolites, as well as fractionated rocks of these series from the metamorphic sole rocks of the Tauride Belt Ophiolites are probably generated in the SSZ environment, as can be observed in the Lau and Mariana Trough from Western Pacific or in the South Sandwich arc-basin system of South Atlantic ocean.

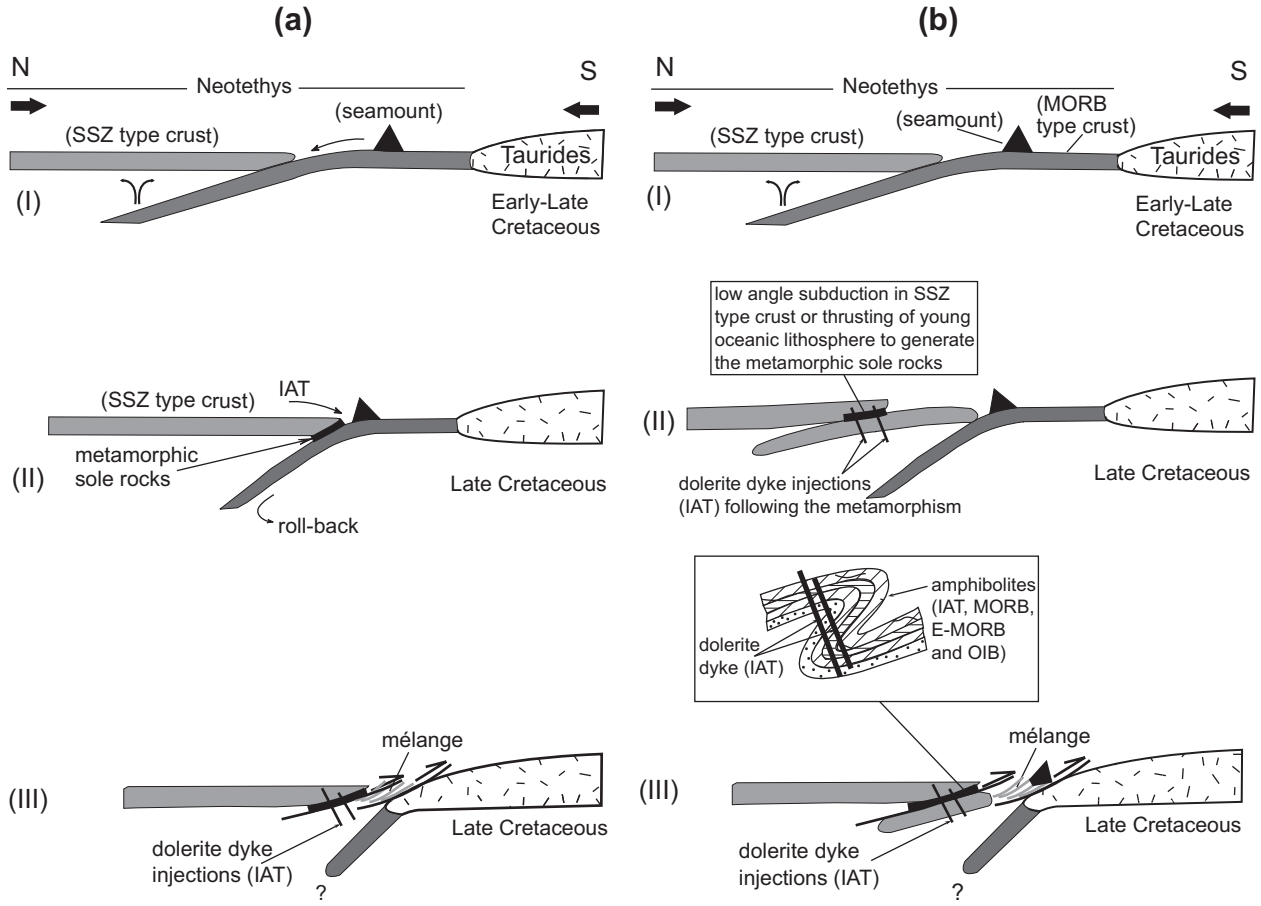

Figure 8. (a) Tectonic model for the generation of the metamorphic sole rocks and their cross-cutting mafic dykes from the Tauride Belt ophiolites (modified after Parlak *et al.* 2006); (b) alternative tectonic diagram illustrating a double subduction model for the generation of the metamorphic sole rocks and cross-cutting mafic dykes from the Tauride Belt ophiolites.

Previous models for generation of the metamorphic sole rocks and their mafic dykes, as well as the Tauride Belt Ophiolites in the Neotethyan ocean envisaged only one subducted oceanic lithosphere (Lytwyn & Casey 1995; Polat *et al.* 1996; Parlak & Delaloye 1996, 1999; Önen & Hall 2000). Most of these studies did not explain the IAT-like amphibolites in the metamorphic sole rocks, and instead generally mentioned amphibolites with OIB and MORB geochemical signatures. IAT-like amphibolites in the metamorphic sole rocks were recently reported by Çelik (2007), Çelik & Delaloye (2003, 2006), and Parlak *et al.* (2006), who identified IAT-like amphibolites in the metamorphic sole rocks of the Divriği ophiolite. They suggested that during intraoceanic subduction (Figure 8a, i), protoliths of the IAT-like amphibolites detached from the front of the overriding SSZ-type crust and protoliths of the OIB-like amphibolites from the top of the subducting plate were initially subducted and metamorphosed up to amphibolite facies (Figure 8a, ii). In their tectonic model, it seems difficult to subduct the protoliths of IAT-like amphibolites into the subduction zone if they remain part of the younger and buoyant oceanic lithosphere. As mentioned earlier, the age of the metamorphic sole rocks is around 92 Ma and the oldest age data obtained from the dolerite dykes for the Mersin ophiolite yields 91.0 ± 0.6 Ma, so the formation ages of the two different rock types are very close (~ 1 or 2 Ma) to one another. Although the metamorphic sole rocks show highly ductile deformation (e.g. folding structures), the cross-cutting dolerite dykes do not (Figure 8b, iii). This means that, when the metamorphic sole rocks were intruded by the dolerite dykes, they were no longer in a metamorphic environment. The dolerite dykes cross-cutting the metamorphic sole rocks in all the Tauride Belt ophiolites show neither ductile

deformation nor metamorphism. The metamorphic pressure estimation (~5 kb) suggests depths of around 17 km. Accordingly, the metamorphic sole rocks were tectonically exhumed from ~17 km towards the oceanic floor before extensive dyke injections in the Neotethyan ocean. In the commonly accepted tectonic model, IAT-like dyke injections into the metamorphic sole rocks (not shown in the model of Parlak *et al*. 2006) should be generated via roll-back and retreat of the subducted lithosphere (Figure 8a, iii). However, it is unclear whether the time period between the two events (1–2 Ma) is sufficient for the exhumation of the metamorphic sole rocks and for the roll-back and retreat of the subducted lithosphere allowing dolerite dyke injection into the metamorphic sole rocks.

OIB-, IAT- and MORB-like geochemistry from the metamorphic sole rocks were exclusively observed together in the same section and at the base of the Lycian ophiolites in the Köyceğiz area (Çelik & Delaloye 2003; Çelik *et al*. 2006). This is very important field evidence from the metamorphic sole rocks that proves that their protoliths were accreted and metamorphosed together beneath the same oceanic lithosphere. The age data from the metamorphic sole rocks also supports their metamorphism at the same time. The cooling and/or generation ages of the metamorphic sole rocks exhibiting IAT-, MORB- and OIB-like geochemistry are similar (Çelik 2002) and range from 91 to 93 Ma (Parlak *et al.* 1995; Dilek *et al*. 1999; Parlak & Delaloye 1999; Çelik *et al*. 2006). These age data also suggest that the SSZ-type ophiolite generation in the Neotethyan ocean is older (> 93 Ma) than that of the metamorphic sole rocks, since there are 93 Ma IAT-like amphibolites in the Lycian ophiolites. As the weakest part of the SSZ, the axial ridge of the backarc basin would be emplaced as young, hot, ocean crust on a low-angle thrust over colder ocean crust and set up conditions for inverted metamorphic gradients on the sole of the thrust zone (Hawkins 2003). Geothermobarometric studies for the metamorphic sole rocks from the Mersin ophiolite suggest that the metamorphic temperature during the metamorphism was 522 ± 15 °C and the pressure was less than 5 kb. Mineral paragenesis and mineral chemistry both show that the metamorphic sole rocks from the Tauride Belt ophiolites were metamorphosed in the amphibolite facies (Parlak *et al*. 1995, 2006; Çelik & Delaloye 2006; Çelik 2002, 2007). Moreover, absence of eclogite or any high-grade metamorphic rocks in the metamorphic sole rocks of the Tauride Belt ophiolites suggest a low-angle of subduction or thrusting in the SSZ environment. Hence, protoliths of the IAT-like amphibolites, together with OIB- and MORB-like amphibolites would all be metamorphosed in the SSZ environment following low-angle subduction or thrusting of the hot oceanic lithosphere on to the relatively cool upper part of the underlying oceanic lithosphere (Figure 8b, ii). As mentioned above, the unmetamorphosed dolerite dykes cutting the metamorphic sole rocks of the Mersin ophiolite were emplaced after the generation of the metamorphic sole rocks. As the metamorphic sole rocks formed in subducted oceanic lithosphere, probably belonging to the SSZ, the dolerite dykes with IAT chemistry should be derived from the older subducted slab which also generated SSZ-type ophiolites (Figure 8b, ii, iii). Therefore, the dolerite dykes exhibiting IAT chemistry provide further evidence for double subduction in the Neotethyan ocean.

Acknowledgments

The author thanks Michel Delaloye and Luis Fontbote for making available laboratory facilities at the University of Geneva, Switzerland. The author thanks Fabio Capponi for performing major and trace element analyses. Osman Parlak is thanked for fruitful discussions in the field. Guidance by Georges Moritz during the microprobe analyses at the University of Lausanne is greatly appreciated. John A. Winchester edited the English of the final text.

References

Avşar, N. 1992. Namrun (İçel) yöresi Paleojen bentik foraminifer faunası [Palaeogene benthic foraminifera fauna of Namrun (İçel) region]. *Mineral Research and Exploration Institute (MTA) of Turkey Bulletin* **114**, 127–144.

Bağcı, U. & Parlak, O. 2006. Geochemical character and tectonic environment of ultramafic to mafic cumulate rocks from the Tekirova (Antalya) ophiolite (southern Turkey). *Geological Journal* **41**, 193–219.

Beccaluva, L., Ohnenstetter, D. & Ohnenstetter, M. 1979. Geochemical discrimination between ocean-floor and island-arc tholeiites-application to some ophiolites. *Canadian Journal of Earth Sciences* **16**, 1874–1872.

Brown, M. 1977. The crossite content of Ca-amphiboles as a guide to pressure of metamorphism. *Journal of Petrology* **18**, 53–72.

ÇELİK, Ö.F. 2002. *Geochemical, Petrological and Geochronological Observations on the Metamorphic Rocks of the Tauride Belt Ophiolites (S. Turkey).* PhD Thesis. Terre & Environment **39**. University of Geneva, Switzerland.

ÇELİK, Ö.F. 2007. Metamorphic sole rocks and their mafic dykes in the eastern Tauride belt ophiolites (southern Turkey): implications for OIB type magma generation following slab break–off. *Geological Magazine* **144**, 849–866.

ÇELİK, Ö.F. & CHIARADIA, M. 2008. Geochemical and petrological aspects of dike intrusions in the Lycian ophiolites (SW Turkey): a case study for the dike emplacement along the Tauride Belt Ophiolites. *International Journal of Earth Sciences* doi:10.1007/s00531-007-0204-0.

ÇELİK, Ö.F. & DELALOYE, M. 2003. Origin of metamorphic sole rocks and their postkinematic mafic dyke swarms in the Antalya and Lycian ophiolites, SW Turkey. *Geological Journal* **38**, 235–256.

ÇELİK, Ö.F. & DELALOYE, M. 2006. Characteristics of ophiolite-related metamorphic rocks in the Beyşehir ophiolitic mélange (Central Taurides, Turkey), deduced from whole rock and mineral chemistry. *Journal of Asian Earth Sciences* **26**, 461–476.

ÇELİK, Ö.F., DELALOYE, M. & FERAUD, G. 2006. Precise ^{40}Ar-^{39}Ar ages from the metamorphic sole rocks of the Tauride Belt Ophiolites, southern Turkey: implications for the rapid cooling history. *Geological Magazine* **143**, 213–227.

DİLEK, Y. & MOORES, E. 1990. Regional tectonics of the eastern Mediterranean ophiolites. *In*: MALPAS, J., MOORES, E., PANAYIOTOU, A. & XENOPHONTOS, C. (eds), *Proceedings of International Troodos Ophiolite Symposium on Ophiolites-oceanic Crustal Analogues*, 295–309.

DİLEK, Y., THY, P., HACKER, B. & GRUNDVIG, S. 1999. Saructure and petrology of Tauride ophiolites and mafic dyke intrusions (Turkey): implications for the Neotethyan ocean. *Geological Society of America Bulletin* **111**, 1192–1216.

ELİTOK, Ö. 2001. Geochemistry and tectonic significance of the Şarkikaraağaç Ophiolite in the Beyşehir-Hoyran Nappes, SW Turkey. *In*: AKINCI, Ö., GÖRMÜŞ, M., KUŞCU, M., KARAGÜZEL, R. & BOZCU, M. (eds), *Proceedings of 4th International Symposium on Eastern Mediterranean Geology*, Isparta, 181–196.

EWART, A. & HAWKESWORTH, C.F. 1987. The Pleistocene–Recent Tonga-Kermadec arc lavas: interpretation of new isotopic and rare earth data in terms of a depleted mantle source model. *Journal of Petrology* **28**, 495–530.

FONTEILLES, M. 1976. *Essai d'interpretation des compositions chimiques des roches d'origine métamorphique et magmatique du massif hercynien de l'Agly, Pyrénées orientales.* PhD Thesis, Université de Paris.

FRETZDORFF, S., LIVERMORE, R.S., DEVEY, C.W., LEAT, P.T. & STOFFERS, P. 2002. Petrogenesis of the back-arc East Scotia Ridge, south Atlantic Ocean. *Journal of Petrology* **43**, 1435–1467.

GRIBBLE, R.F., STERN, R.J., BLOOMER, S.H., NEWMAN, S. & O'HEARN, T. 1988. Chemical and isotopic composition of lavas from the northern Mariana Trough: implications for magma genesis in backarc basins. *Journal of Petrology* **39**, 122–154.

GRIBBLE, R.F., STERN, R.J., BLOOMER, S.H., STUBEN, D.H., O'HEARN, T. & NEWMAN, S. 1996. MORB mantle and subduction components interact to generate basalts in the southern Mariana Trough back-arc basin. *Geochimica et Cosmochimica Acta* **60**, 2153–2166.

HARRISON, T.M. 1981. Diffusion of ^{40}Ar in hornblende. *Contributions to Mineralogy and Petrology* **78**, 324–331.

HAWKINS, J.W. 1976. Petrology and geochemistry of basaltic rocks of the Lau basin. *Earth and Planetary Science Letters* **28**, 283–298.

HAWKINS, J.W. 1995a. The geology of the Lau Basin. *In*: TAYLOR, B. (ed) *Backarc Basins: Tectonics and Magmatism.* New York Plenum Press, 63–138.

HAWKINS, J.W. 1995b. Evolution of the Lau Basin - insights from ODP Leg 135. *In*: TAYLOR, B. & NATLAND, J. (eds). *Active Margins and Marginal Basins of the Western Pasific*. American Geophysical Union Monograph **88**, 126–174.

HAWKINS, J.W. 2003. Geology of supra-subduction zones – implications for the origin of ophiolites. *In*: DILEK, Y. & NEWCOMB, S. (eds), *Ophiolite Concept and the Evolution of Geological Thought*. The Geological Society of America Special Paper **373**, 227–268.

HAWKINS, J.W. & MELCHIOR, J.T. 1985. Petrology of Mariana Trough and Lau basin basalts. *Journal of Geophysical Research* **90**, 11431–11468.

HAWKINS, J.W., LONSDALE, P.F., MACDOUGALL, J.D. & VOLPE, A.M. 1990. Petrology of the axial ridge of the Mariana Trough backarc spreading center. *Earth and Planetary Science Letters* **100**, 226–250.

HOLLAND, T.J.B. & BLUNDY, J.D. 1994. Non-Ideal interactions in calcic amphiboles and their bearing on amphibole-plagioclase thermometry. *Contributions to Mineralogy and Petrology* **116**, 433–447.

IKEDA, Y. & YUASA, M. 1989. Volcanism in nascent back-arc basins behind the Shichito Ridge and adjacent areas in the Izu-Ogasawara arc, northwest Pacific: evidence for mixing between E-Type MORB and island arc magmas at the initiation of back-arc rifting. *Contributions to Mineralogy and Petrology* **101**, 377–393.

JOHNSON, M.C. & PLANK, T. 1999. Dehydration and melting experiments constrain the fate of subducted sediments. *Geochemistry, Geophysics, Geosystems* **1**, 1999GC000014.

JUTEAU, T. 1980. Ophiolites of Turkey. *Ofioliti* **2**, 199–235.

KOEPKE, J., SEIDEL, E. & KREUZER, H. 2002. Ophiolites on the Southern Aegean islands Crete, Karpathos and Rhodes: composition, geochronology and position within the ophiolite belts of the Eastern Mediterranean. *Lithos* **65**, 183–203.

LAIRD, J., LANPHERE, A. & ALBEE, A.L. 1984. Distribution of Ordovician and Devonian metamorphism in mafic and pelitic schists from Vermont. *American Journal of Science* **284**, 376–416.

LEAKE, B.E. 1964. The chemical distinction between ortho- and para-amphibolites. *Journal of Petrology* **5**, 238–254.

LEAKE, B.E., WOOLLEY, A.R., ARPS, C.E.S., BIRCH, W.D., GILBERT, M.C., GRICE, J.D., HAWTHOPNE, F.C., KATO, A., KISCH, H.J., KRIVOVICHEV, V.G., LINTHOUT, K., LAIRD, J., MANDARINO, J., MARESCH, W.V., NICKEL, E.H., ROCK, N.M.S., SCHUMACHER, J.C., SMITH, D.C., STEPHENSON, N.C.N., UNGARETTI, L., WHITTAKER, E.J.W. & YOUZHI, G. 1997. Nomenclature of amphiboles: Report of the subcommitee on amphiboles of the International Mineralogical Association, commission on new minerals and mineral names. *American Mineralogist* **82**, 1019–1037.

LEAT, P.T., LIVERMORE, R.A., MILLAR, I.L. & PEARCE, J.A. 2000. Magma supply in back-arc spreading centre segment E2, East Scotia Ridge. *Journal of Petrology* **41**, 845–866.

LEAT, P.T., PEARCE, J.A., BARKER, P.F., MILLAR, I.L., BARRY, T.L. & LARTER, R.D. 2004. Magma genesis and mantle flow at a subducting slab edge: the South Sandwich arc-basin system. *Earth and Planetary Science Letters* **227**, 17–35.

LYTWYN, J.N. & CASEY, J.F. 1995. The geochemistry of postkinematic mafic dyke swarms and subophiolitic metabasites, Pozantı-Karsantı ophiolite, Turkey: evidence for ridge subduction. *Geology Society of America Bulletin* **7**, 830–850.

MULLEN, E.D. 1983. $MnO/TiO_2/P_2O_5$: a minor element discriminant for basaltic rocks of oceanic environnement and its implication for petrogenesis. *Earth and Planetary Science Letters* **62**, 53–62.

ÖNEN, A.P. & HALL, R. 2000. Sub-ophiolite metamorphic rocks from NW Anatolia, Turkey. *Journal of Metamorphic Geology* **18**, 483–495.

PARLAK, O. 1996. *Geochemistry and Geochronology of the Mersin Ophiolite within the Eastern Mediterranean Tectonic Frame.* PhD Thesis. Terre & Environnement **6**, University of Geneva, Switzerland.

PARLAK, O. & DELALOYE, M. 1996. Geochemistry and timing of post-metamorphic dyke emplacement in the Mersin ophiolite (southern Turkey): new age constraints from $^{40}Ar/^{39}Ar$ geochronology. *Terra Nova* **8**, 585–592.

PARLAK, O. & DELALOYE, M. 1999. Precise ^{40}Ar-^{39}Ar ages from the metamorphic sole of the Mersin ophiolite (Southern Turkey). *Tectonophysics* **301**, 145–158.

PARLAK, O., DELALOYE, M. & BİNGÖL, E. 1995. Origin of sub-ophiolitic metamorphic rocks beneath the Mersin ophiolite, southern Turkey. *Ofioliti* **20**, 97–110.

PARLAK, O., DELALOYE, M. & BİNGÖL, E. 1996. Mineral chemistry of ultramafic and mafic cumulates as an indicator of arc-related origin of the Mersin ophiolite (southern Turkey). *Geologische Rundschau* **85**, 647–661.

PARLAK, O., HÖCK, V. & DELALOYE, M. 2000. Suprasubduction zone origin of the Pozantı-Karsantı Ophiolite (Southern Turkey) deduced from whole-rock and mineral chemistry of the gabbroic cumulates. *In*: BOZKURT, E., WINCHESTER, J.A. & PIPER, J.D.A. (eds), *Tectonics and Magmatism in Turkey and the Surrounding Area*. Geological Society, London, Special Publications **173**, 219–234.

PARLAK, O., HÖCK, V. & DELALOYE, M. 2002. The supra-subduction zone Pozantı-Karsantı ophiolite, southern Turkey: evidence for high-pressure crystal fractionation of ultramafic cumulates. *Lithos* **65**, 205–224.

PARLAK, O. & ROBERTSON, A.H.F. 2004. Tectonic setting and evolution of the ophiolite-related Mersin Mélange, southern Turkey: its role in the tectonic-sedimentary setting of the Tethys in the eastern Mediterranean region. *Geological Magazine* **141**, 257–286.

PARLAK, O., YILMAZ, H. & BOZTUĞ, D. 2006. Origin and tectonic significance of the metamorphic sole and isolated dykes of the Divriği ophiolite (Sivas, Türkiye): evidence for slab break-off prior to ophiolite emplacement. *Turkish Journal of Earth Sciences* **15**, 25–45.

PEARCE, J.A. 1980. Geochemical evidence for the genesis and eruptive setting of lava from Tethyan ophiolites. *In*: PANAYIOTOU, A. (ed), *Ophiolites*. Cyprus, 299–317.

PEARCE, J.A. 1982. Trace element characteristicns of lavas from destructive plate boundaries. *In*: THORPE, R.S. (ed), *Andesites.* Wiley and Sons, New York, 525–548.

PEARCE, J.A. 2003. Supra-subduction zone ophiolites: the search for modern analogues. *In*: DILEK, Y. & NEWCOMB, S. (eds), *Ophiolite Concept and the Evolution of Geological Thought*. The Geological Society of America Special Paper **373**, 269–293.

PEARCE, J.A., LIPPARD, S.J. & ROBERTS, S. 1984. Characteristics and tectonic significance of supra-subduction zone ophiolites. *In*: KOKELAAR, B.P. & HOWELS, M.F. (eds), *Marginal Basin Geology.* Geological Society, London, Special Publications **16**, 77–94.

PEARCE, J.A., ALABASTER, T., SHELTON, A.W. & SEARLE, M.P. 1981. The Oman ophiolite as a Cretaceous arc-basin complex: evidence and implications. *Philosophical Transactions Royal Society of London* **300**, 299–317.

PEARCE, J.A., BARKER, P.F., EDWARDS, S.J., PARKINSON, I.J. & LEAT, P.T. 2000. Geochemistry and tectonic significance of peridotites from the South Sandwich arc-basin system, South Atlantic. *Contributions to Mineralogy and Petrology* **139**, 36–53.

POLAT, A., CASEY, J.F. & KERRICH, R. 1996. Geochemical characteristics of accreted material beneath the Pozantı-Karsantı ophiolite, Turkey: Intra-oceanic detachment, assembly and obduction. *Tectonophysics* **263**, 249–276.

RAASE, P. 1974. Al and Ti contents of hornblende, indicators of pressure temperature of regional metamorphism. *Contributions to Mineralogy and Petrology* **45**, 231–236.

ROBERTSON, A.H.F. 2002. Overview of the genesis and emplacement of Mesozoic ophiolites in the Eastern Mediterranean Tethyan region. *Lithos* **65**, 1–67.

SAUNDERS, A.D. & TARNEY, J. 1979. The geochemistry of basalts from a back-arc spreading centre in the East Scotia Sea. *Geochimica Cosmochimica Acta* **43**, 555–572.

SAUNDERS, A.D. & TARNEY, J. 1984. Geochemical characteristics of basaltic volcanism within back-arc basins. *In*: KOKELAAR, B.P. & HOWELLS, M.F. (eds), *Marginal Basin Geology*. Geology Society, London, Special Publications **16**, 59–76.

SHERVAIS, W.J. 1982. Ti-V plots and the petrogenesis of modern and ophiolitic lavas. *Earth and Planetary Science Letters* **59**, 102–118.

STEIGER, R.H. & JÄEGER, E. 1977. Subcommission on geochronology: convention on the use of decay constants in geo-and cosmochronology. *Earth and Planetary Science Letters* **55**, 359–362.

SUN, S.S. & MC DONOUGH, W.F. 1989. Chemical and isotopic systematics of oceanic basalts: Implications for mantle composition and processes. *In*: SAUNDERS, A.D. & NORRY, M.J. (eds), *Magmatism in the Ocean Basins*. Geological Society, London, Special Publications **42**, 313–345.

THOMPSON, G. 1991. Metamorphic and hydrothermal processes: basalt-seawater interactions. *In*: FLOYD, P.A. (ed), *Oceanic Basalts.* Blackie, Glasgow, 148–173.

THUIZAT, R., WHITECHURCH, H., MONTIGNY, R. & JUTEAU, T. 1981. K-Ar dating of some infra-ophiolitic metamorphic soles from the eastern Mediterranean: New evidence for oceanic thrusting before obduction. *Earth and Planetary Science Letters* **52**, 302–310.

TINDLE, A.G. & WEBB, P.C. 1994. PROBE-AMPH a spreadsheet program to classify microprobe-derived amphibole analyses. *Computers and Geosciences* **20**, 1201–1228.

VERGİLİ, Ö. & PARLAK, O. 2005. Geochemistry and tectonic setting of metamorphic sole rocks and mafic dykes from the Pınarbaşı (Kayseri) ophiolite, Central Anatolia (Turkey). *Ofioliti* **30**, 37–52.

VOLPE, A.M., MACDOUGALL, J.D., LUGMAIR, G., HAWKINS, J.W. & LONSDALE, P.F. 1990. Fine-scale isotropic variation in Mariana Trough basalts: evidence for heterogeneity and recycled component in backarc basin mantle. *Earth and Planetary Science Letters* **100**, 251–264.

Received 17 September 2007; revised typescript received 22 February 2008; accepted 31 March 2008